J. Fluid Mech. (2013), *vol.* 736, *pp.* 5–43. © Cambridge University Press 2013
doi:10.1017/jfm.2013.521

Unifying binary fluid diffuse-interface models in the sharp-interface limit

David N. Sibley, Andreas Nold and Serafim Kalliadasis†

Department of Chemical Engineering, Imperial College London, London SW7 2AZ, UK

(Received 11 January 2013; revised 16 August 2013; accepted 26 September 2013;
first published online 1 November 2013)

Recent results published by Gugenberger *et al.* on surface diffusion (*Phys. Rev.* E, vol. 78, 2008, 016703), show that the sharp-interface limit of the phase field models often adopted in the literature fails to produce the appropriate boundary conditions. With this knowledge, we consider the sharp-interface limit of phase field models for binary fluids, obtained carefully, where hydrodynamic equations are coupled to phase field evolution based on Cahn–Hilliard or Allen–Cahn theories, in a variety of guises, and unify and contrast their forms and behaviours in the sharp-interface limit. In particular, a tensorial mobility model is analysed, which allows the bulk fluids in the outer region to satisfy classical Navier–Stokes type equations to all orders in the Cahn number.

Key words: general fluid mechanics, interfacial flows (free surface), multiphase flow

1. Introduction

Flows involving free boundaries occur widely in both nature and technological applications, from climate modelling and haemodynamics (study of blood flow) to oil extraction and polymer processing. The challenge of tracking an evolving free surface coupled to complex hydrodynamics has been well known for many years, with the study of capillarity and the understanding of surface tension starting from the work of Laplace (1805) and Young (1805) at the beginning of the 19th century.

In recent years analytical and numerical techniques have advanced sufficiently so that flows from the microscale to the global scale can be modelled and accurate predictions made; for reviews of analytical and numerical simulation of free-surface flows see Eggers (1997) and Scardovelli & Zaleski (1999), while the classical governing equations and boundary conditions are summarized in figure 1. Of central interest to this study is an approach which considers the interface between two ostensibly immiscible fluids, such as oil and water and termed a binary fluid, to have a thin but finite thickness. In this case quantities such as the mass fraction of the two fluid components are modelled as varying smoothly but rapidly in the interfacial region, with the classical hydrodynamic model and free-surface boundary conditions recovered in the sharp-interface limit, as the interface thickness goes to zero. These 'diffuse-interface models', through gradients of the chemical potential of the system in their thin interfacial region, allow diffusion to occur between the two fluid components.

† Email address for correspondence: s.kalliadasis@imperial.ac.uk

https://doi.org/10.1017/jfm.2013.521 Published online by Cambridge University Press

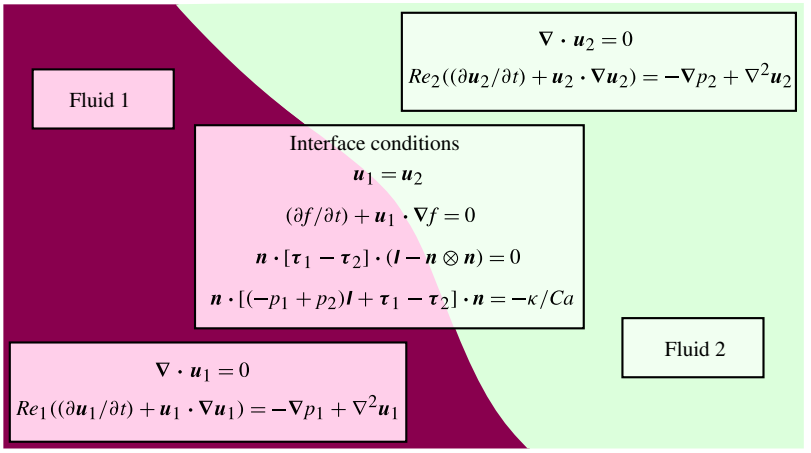


FIGURE 1. (Colour online) The classical model for the bulk and free-surface conditions for two Newtonian viscous fluids, where $f(\boldsymbol{r}, t) = 0$ is the equation of the moving interface separating fluid 1, where $f > 0$, and fluid 2, where $f < 0$. Other notational definitions can be found in § 2.

The foundations of diffuse-interface models can be traced to van der Waals (1893) (English translation by Rowlinson 1979) and Korteweg (1901) (see the review by Anderson, McFadden & Wheeler 1998), whose constitutive law forming the capillary (or Korteweg) stress tensor forms part of a well-used diffuse-interface model for liquid–gas systems (Seppecher 1996; Pismen & Pomeau 2000). For binary fluids, the work of Cahn & Hilliard (1958) considering a fluid undergoing spinodal decomposition provided an equation to model the evolution of the composition of the fluid, which forms the basis of the models here when coupled with equations to model the hydrodynamic behaviour.

In the literature there have been a number of similar models used to consider binary fluids, such as those in Jacqmin (1999, 2000), Yang *et al.* (2006), Khatavkar, Anderson & Meijer (2006), Ding & Spelt (2007), Yue, Zhou & Feng (2010) and more recently Magaletti *et al.* (2013). Whilst many of these models are used predominantly for their numerical convenience, when they are applied to situations where physical length scales are comparable to the diffuse-interface width or when the Cahn–Hilliard diffusion is an important physical effect (such as in moving contact line problems), the particular model and the understanding of the interfacial region becomes critical (Yue *et al.* 2010).

Here, we consider asymptotically the sharp-interface limit of these various models, alongside extensions motivated by the recent results of Gugenberger, Spatschek & Kassner (2008) for phase field models for surface diffusion (where hydrodynamics are not included), to clarify various features of the models. Figure 2 contains a general model which contains all forms studied here, and shows the sections in which they will be considered. Another summary of models, formulated as a general model with modified pressures, is discussed in appendix A. The purpose of this work is to unify the range of different models through the analysis of their equations in the sharp-interface limit, and to highlight the benefit of a modification to tensorial form of the mobility of the commonly used CH model, the model with $(\mathscr{B}, \mathscr{C}) = (0, 1)$, $\gamma_i = 1$, $\alpha = 0$ in figure 2. Although all of the conservative models here have a phase

https://doi.org/10.1017/jfm.2013.521 Published online by Cambridge University Press

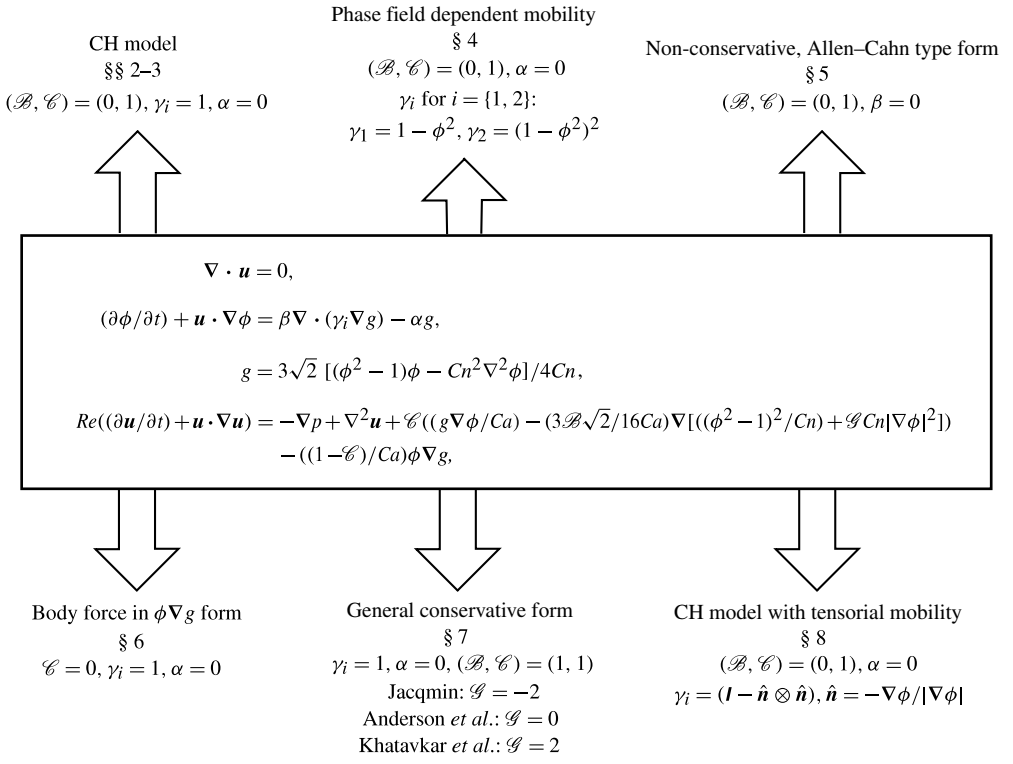


FIGURE 2. Schematic with the various binary fluid models, in non-dimensional form, considered in this study, and combined into a single system of equations for ease of comparison.

field evolution equation motivated by the work of Cahn & Hilliard (1958), we term this the CH model for convenience (noting that it is closely related to model H in the terminology of Hohenberg & Halperin 1977). A tensorial form of the mobility where diffusion is preferred tangential to the interface, a physically reasonable suggestion for ostensibly immiscible fluids, allows the classical Navier–Stokes equations to be recovered to any order in the non-dimensional Cahn number, in the limit as it tends to zero (the sharp-interface limit), whereas the usual constant or scalar mobility forms of the CH model have non-classical terms at $O(Cn)$.

2. Problem specification

2.1. *Governing equations*

We consider two ostensibly immiscible Newtonian fluids in contact with each other, and introduce an order parameter ϕ representing a scaled 'concentration' such that the two bulk fluids satisfy $\phi=\pm1$ and the fluid–fluid interface is given by $\phi=0$. Considering the fluid domain Ω, we model the system with a free energy based on the Ginzburg–Landau formulation

$$\breve{\mathscr{F}}=\int_\Omega \breve{f}_m(\phi,\breve{\nabla}\phi)\,\mathrm{d}\Omega=\int_\Omega\left[\frac{\lambda}{2}|\breve{\nabla}\phi|^2+\frac{\lambda}{4\epsilon^2}(\phi^2-1)^2\right]\mathrm{d}\Omega, \tag{2.1}$$

https://doi.org/10.1017/jfm.2013.521 Published online by Cambridge University Press

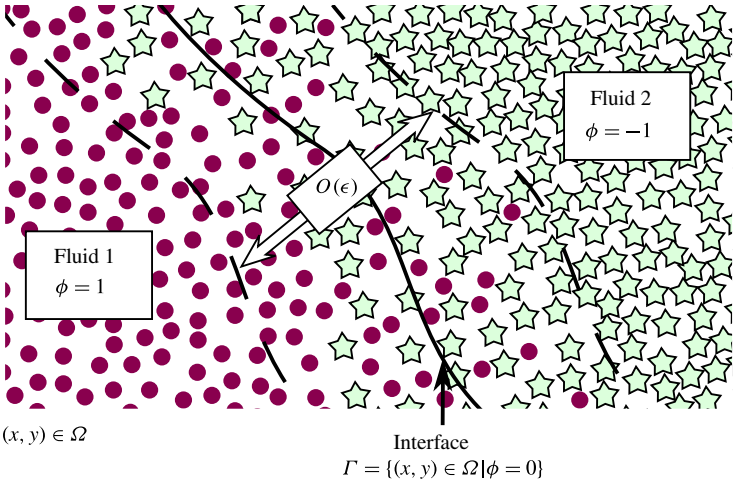


FIGURE 3. (Colour online) Schematic representation of the two fluids with bulk phase field values $\phi = \pm 1$, interface defined by $\phi = 0$, and with interfacial width of $O(\epsilon)$.

where $\breve{f}_m$ is the fluid–fluid mixing energy (Cahn & Hilliard 1958), and we note that dimensional variables are represented with a breve diacritical mark, e.g. $\breve{\mathscr{F}}$, to distinguish them from their non-dimensional counterparts later. The terms in (2.1) are a square gradient term and a double-well potential, defining an interface of (capillary) width ϵ and with mixing energy density λ. Through a variational procedure we find the chemical potential

$$\breve{g} = \frac{\delta \breve{\mathscr{F}}}{\delta \phi} = \frac{\partial \breve{f}_m}{\partial \phi} - \breve{\boldsymbol{\nabla}} \cdot \frac{\partial \breve{f}_m}{\partial \breve{\boldsymbol{\nabla}} \phi} = \lambda \left[\frac{(\phi^2 - 1)\phi}{\epsilon^2} - \breve{\nabla}^2 \phi \right], \tag{2.2}$$

and at equilibrium (minimizing $\breve{\mathscr{F}}$: see Yue *et al.* 2004) the fluid–fluid interfacial tension σ is calculated as

$$\sigma = \lambda \int_{-\infty}^{\infty} \left(\frac{\mathrm{d}\phi}{\mathrm{d}\breve{z}} \right)^2 \mathrm{d}\breve{z} = \frac{2\sqrt{2}}{3} \frac{\lambda}{\epsilon}. \tag{2.3}$$

A schematic of the diffuse-interface model for a binary fluid is shown in figure 3, where the interface, of thickness $O(\epsilon)$, in which diffusion occurs is also shown.

The effect of the free energy is coupled to the usual Navier–Stokes equations through a 'body force', of which we will consider a number of forms from the literature. Initially, as considered by Qian, Wang & Sheng (2006), Ding & Spelt (2007), Ding, Spelt & Shu (2007) and Yue *et al.* (2010), we consider the form $\breve{\boldsymbol{b}} = \breve{g} \breve{\boldsymbol{\nabla}} \phi$, the diffuse-interface equivalent of the interfacial tension. In the cited works, alongside many others, the phase field ϕ satisfies a Cahn–Hilliard equation (conserved phase field), and with this body force, forms the CH model. An alternative to this is for the phase field to be described by a non-conservative Allen–Cahn type equation, with some careful adaptations to enforce the conservation of the volume fractions through other means. Whilst detailed analysis of the works using corrective terms to enforce conservation of mass based on the Allen–Cahn equation are outside the scope of the present manuscript, we will analyse a simple Allen–Cahn/Navier–Stokes

https://doi.org/10.1017/jfm.2013.521 Published online by Cambridge University Press

model (which does not enforce conservation of the volume fractions but is used in appropriate circumstances such as in reactive wetting with intermetallic formation: Villanueva *et al.* 2012) in § 5 to provide motivation for considering, in the later sections, more involved mobilities and body forces than that of the CH model.

The system of equations for the CH model is thus

$$\breve{\boldsymbol{\nabla}} \cdot \breve{\boldsymbol{v}} = 0, \tag{2.4}$$

$$\rho \left(\frac{\partial \breve{\boldsymbol{v}}}{\partial \breve{t}} + \breve{\boldsymbol{v}} \cdot \breve{\boldsymbol{\nabla}} \breve{\boldsymbol{v}} \right) = -\breve{\boldsymbol{\nabla}} \breve{p} + \breve{\boldsymbol{\nabla}} \cdot \breve{\boldsymbol{\tau}} + \breve{g} \breve{\boldsymbol{\nabla}} \phi, \tag{2.5}$$

with the Cahn–Hilliard type equation

$$\frac{\partial \phi}{\partial \breve{t}} + \breve{\boldsymbol{v}} \cdot \breve{\boldsymbol{\nabla}} \phi = \breve{\boldsymbol{\nabla}} \cdot (\gamma \breve{\boldsymbol{\nabla}} \breve{g}), \tag{2.6}$$

or the non-conservative Allen–Cahn type equation

$$\frac{\partial \phi}{\partial \breve{t}} + \breve{\boldsymbol{v}} \cdot \breve{\boldsymbol{\nabla}} \phi = -\mathscr{A} \breve{g}. \tag{2.7}$$

Here $\breve{\boldsymbol{\tau}} = 2\mu \breve{\boldsymbol{D}} = \mu[(\breve{\boldsymbol{\nabla}} \breve{\boldsymbol{v}}) + (\breve{\boldsymbol{\nabla}} \breve{\boldsymbol{v}})^{\mathrm{T}}]$ is the viscous stress tensor, $\breve{\boldsymbol{v}}$ is the fluid velocity, $\breve{p}$ is the pressure, $\breve{\boldsymbol{D}}$ is the rate of strain tensor as defined, and μ and ρ are the fluid viscosities and densities, respectively, which are taken to be equal for simplicity, but including phase field dependence will not change the analysis. For example, these could be defined as algebraic averages along the same lines as Yue *et al.* (2006), with

$$\{\mu, \rho\} = \frac{1+\phi}{2} \{\mu_1, \rho_1\} + \frac{1-\phi}{2} \{\mu_2, \rho_2\}, \tag{2.8}$$

so that the viscosity and density vary in proportion to the phase field from fluid 1 (with viscosity μ_1 and density ρ_1) to fluid 2 (with viscosity μ_2 and density ρ_2). In other studies, such as those of Liu & Shen (2003) and Khatavkar, Anderson & Meijer (2007), the densities and/or viscosities are taken as harmonic averages, e.g. for the density

$$\frac{1}{\rho(\phi)} = \frac{1+\phi}{2\rho_1} + \frac{1-\phi}{2\rho_2}. \tag{2.9}$$

These are used, since the Cahn–Hilliard equation does not satisfy the maximum principle and hence the algebraic averages cannot be guaranteed to be bounded away from zero, whereas harmonic averages lead to the desired properties, as discussed by Liu & Shen (2003) and in the recent review by Kim (2012).

Finally $\mathscr{A}$ defines a relaxation time scale of the system, based on the chemical potential $\breve{g}$, and γ is a mobility parameter, which will initially be taken as a constant but will later be generalized to either a scalar or tensor function of the phase field, i.e. $\gamma = \gamma(\phi)$.

Indeed, after considering the prevalent version of the binary fluid diffuse-interface model above with the conservative Cahn–Hilliard type equation, and uncovering the drawback that non-classical effects must be present at next to leading order in the sharp-interface limit, we will discuss other binary fluid model forms which are already free of this restriction, before suggesting how to overcome it for this simple model. The various forms include phase field dependent mobility, $\gamma = \gamma(\phi)$, which does not resolve the restriction, and non-conservative models as well as models with more complex diffusion coupling terms to the hydrodynamics, which do.

https://doi.org/10.1017/jfm.2013.521 Published online by Cambridge University Press

2.2. *Non-dimensionalization*

We introduce the scalings

$$\breve{x} = Lx, \quad \breve{y} = Ly, \quad \breve{\boldsymbol{v}} = U\boldsymbol{u}, \quad \breve{t} = \frac{L}{U}t, \quad \breve{p} = \frac{\mu U}{L}, \quad \breve{g} = \frac{\sigma}{L}g, \tag{2.10}$$

where L is a typical macroscopic length scale, U is a typical velocity scale, and we note that ϕ is already non-dimensional. The governing equations will contain the non-dimensional parameters

$$Ca = \frac{\mu U}{\sigma}, \quad Cn = \frac{\epsilon}{L}, \quad \alpha = \frac{\mathscr{A}\sigma}{U}, \quad \beta = \frac{\sigma\gamma}{L^2 U}, \quad Re = \frac{\rho UL}{\mu}. \tag{2.11}$$

These non-dimensional parameters are the usual capillary number (Ca) representing the relative effect of viscous forces and surface tension, the Cahn number (Cn) being the relative size of the interfacial thickness, the non-dimensional mobility parameters for the non-conservative and conservative cases respectively, and the Reynolds number.

The choice of β for non-dimensional mobility has been made for notational simplicity. Two other noteworthy choices are, for example, in Yue *et al.* (2010) (giving the form of the CH model), where a non-dimensional parameter $S = \sqrt{\gamma\mu}/L = \sqrt{\beta Ca}$ is used, and in Khatavkar *et al.* (2006, 2007) (which will be considered in greater detail in § 7), where a Péclet number is defined as $Pe = UL\epsilon/(\gamma\sigma) = Cn\,Ca/S^2 = Cn/\beta$. The form for α is then chosen to be the analogue of β for the non-conservative case.

The equations become

$$\boldsymbol{\nabla}\cdot\boldsymbol{u} = 0, \tag{2.12}$$

$$Re\left(\frac{\partial \boldsymbol{u}}{\partial t} + \boldsymbol{u}\cdot\boldsymbol{\nabla}\boldsymbol{u}\right) = -\boldsymbol{\nabla}p + \nabla^2\boldsymbol{u} + \frac{1}{Ca}g\boldsymbol{\nabla}\phi, \tag{2.13}$$

$$\frac{4}{3\sqrt{2}}Cn\,g = \left[(\phi^2-1)\phi - Cn^2\nabla^2\phi\right], \tag{2.14}$$

with either Cahn–Hilliard type evolution equation

$$\frac{\partial\phi}{\partial t} + \boldsymbol{u}\cdot\boldsymbol{\nabla}\phi = \beta\nabla^2 g, \tag{2.15}$$

or Allen–Cahn type equation for the phase field,

$$\frac{\partial\phi}{\partial t} + \boldsymbol{u}\cdot\boldsymbol{\nabla}\phi = -\alpha g. \tag{2.16}$$

Note that $\boldsymbol{\nabla}\cdot\boldsymbol{\tau} = [\nabla^2\boldsymbol{u} + \boldsymbol{\nabla}(\boldsymbol{\nabla}\cdot\boldsymbol{u})] = \nabla^2\boldsymbol{u}$, where $\boldsymbol{\tau} = (\boldsymbol{\nabla}\boldsymbol{u}) + (\boldsymbol{\nabla}\boldsymbol{u})^{\mathrm{T}}$ is the non-dimensional stress tensor. We now have a set of governing equations to consider. The non-dimensional parameter of most significance in this analysis is the Cahn number, as here we are interested in considering the behaviour of this, and the other models in figure 2, in the sharp-interface limit, when $Cn \to 0$. In this limit we expect the classical equations and boundary conditions to be recovered, depicted in figure 1, through asymptotic analysis to consider the outer, or bulk, regions away from the interface and an inner (interfacial) region with matching to the two bulk regions. It is this that we next consider.

https://doi.org/10.1017/jfm.2013.521 Published online by Cambridge University Press

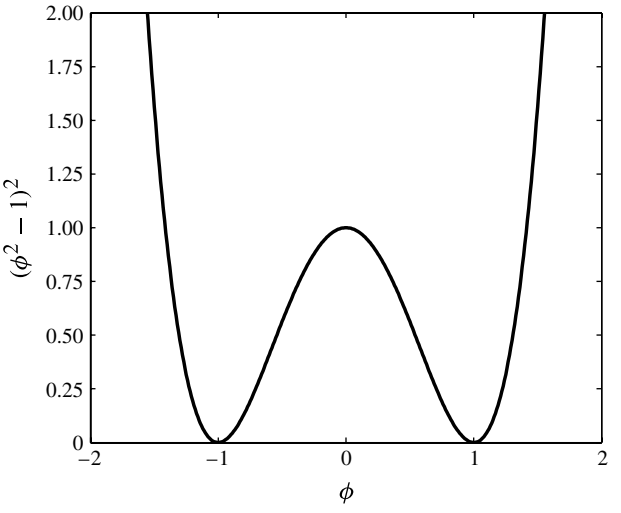


FIGURE 4. Plot of the double-well potential term in the free energy, given in (2.1).

3. Asymptotic analysis

3.1. *The outer region for the CH model*

In the outer region for the bulk fluids away from the interface defined by $\Gamma = \{(t, x, y) \in \Omega | \phi(t, x, y) = 0\}$, we consider the sharp-interface limit by taking $Cn \to 0$ and using the expansions

$$\phi(t,x,y) = \phi_0^{\pm} + Cn\,\phi_1^{\pm} + Cn^2\phi_2^{\pm} + \cdots, \quad g(t,x,y) = g_0^{\pm} + Cn\,g_1^{\pm} + Cn^2 g_2^{\pm} + \cdots, \tag{3.1a}$$

$$\boldsymbol{u}(t,x,y) = \boldsymbol{u}_0^{\pm} + Cn\,\boldsymbol{u}_1^{\pm} + Cn^2\boldsymbol{u}_2^{\pm} + \cdots, \quad p(t,x,y) = p_0^{\pm} + Cn\,p_1^{\pm} + Cn^2 p_2^{\pm} + \cdots, \tag{3.1b}$$

where, for example, ϕ_0^+ is in the region of fluid 1. At leading order we find that $\phi_0^{\pm} = \pm 1$. $\phi_0^{\pm} = 0$ is also a solution of the governing equations, but we may exclude this result as $\phi = 0$ is the equation of the interface and we are considering outer regions away from this, thus a contradiction; further, the zero solution is a local maximum in the double-well potential term of the free energy, and is thus unstable – see figure 4. We also find

$$\nabla \cdot \boldsymbol{u}_0^{\pm} = 0, \tag{3.2}$$

$$Re\left(\frac{\partial \boldsymbol{u}_0^{\pm}}{\partial t} + \boldsymbol{u}_0^{\pm} \cdot \nabla \boldsymbol{u}_0^{\pm}\right) = -\nabla p_0^{\pm} + \nabla^2 \boldsymbol{u}_0^{\pm}, \tag{3.3}$$

$$\nabla^2 g_0^{\pm} = 0, \tag{3.4}$$

the classical Navier–Stokes equations for incompressible fluids, as desired, with a Laplace equation for the leading-order chemical potential.

The following order gives

$$\nabla \cdot \boldsymbol{u}_1^{\pm} = 0, \tag{3.5}$$

$$Re\left(\frac{\partial \boldsymbol{u}_1^{\pm}}{\partial t} + \boldsymbol{u}_0^{\pm} \cdot \nabla \boldsymbol{u}_1^{\pm} + \boldsymbol{u}_1^{\pm} \cdot \nabla \boldsymbol{u}_0^{\pm}\right) = -\nabla p_1^{\pm} + \nabla^2 \boldsymbol{u}_1^{\pm} + \frac{1}{Ca} g_0^{\pm} \nabla \phi_1^{\pm}, \tag{3.6}$$

https://doi.org/10.1017/jfm.2013.521 Published online by Cambridge University Press

$$\frac{\partial \phi_1^{\pm}}{\partial t} + \boldsymbol{u}_0^{\pm} \cdot \boldsymbol{\nabla} \phi_1^{\pm} = \beta \nabla^2 g_1^{\pm}, \tag{3.7}$$

$$\frac{4}{3\sqrt{2}} g_0^{\pm} = \phi_1^{\pm}(3\phi_0^{\pm 2} - 1) = 2\phi_1^{\pm}, \tag{3.8}$$

having used $\phi_0^{\pm} = \pm 1$ to remove some terms already. Now that we have these first two orders, we see that

$$\nabla^2 g_0^{\pm} = 0 \Rightarrow \nabla^2 \left(\frac{3\sqrt{2}}{2} \phi_1^{\pm} \right) = 0 \Rightarrow \nabla^2 \phi_1^{\pm} = 0. \tag{3.9}$$

We require $\phi_1^{\pm} \to 0$ as the distance to the interface increases, but do not have details of $\phi_1^{\pm}$ or $g_0^{\pm}$ as the interface is approached. As $\phi_1^{\pm}$ and $g_0^{\pm}$ are harmonic, with further information about their behaviours at the boundary of these outer regions the maximum principle may then be applied.

We will see that the inner region results will cause $g_0^{\pm} \to \kappa/2$, where κ is the interface curvature, as the interface is approached. This result crucially then determines that for curved interfaces, there must be non-zero non-classical terms at $O(Cn)$ in the outer regions in this CH model (specifically in the last term of (3.6)).

If, however, we have a planar interface with $\kappa = 0$ so that $g_0^{\pm} \to 0$ as the interface is approached, and as the distance tends to infinity, then the maximum principle would force $\phi_1^{\pm} = g_0^{\pm} = 0$. This in turn suggests that linearized versions of the Navier–Stokes equations hold in these bulk regions to both leading and next to leading orders, without the non-classical diffusive effects playing a role.

3.2. *The inner region of the CH model*

We utilize body-fitted coordinates (ζ^1, ζ^2), in a similar fashion to a number of other works (e.g. Caginalp & Fife 1988; Pego 1989; Lowengrub & Truskinovsky 1998; Folch *et al.* 1999; Anderson, McFadden & Wheeler 2001), centred on the interface ($\phi = 0$, given by $\boldsymbol{r} = \boldsymbol{r}_0(\zeta^1, t)$); ζ^1 measures distance along the interface (like an arclength), and ζ^2 measures the distance in the normal direction from the point $(x, y) \in \Omega$ to the interface $\Gamma = \Gamma(t)$. A schematic of these coordinates is shown in figure 5(*a*), and we note an issue with this approach in figure 5(*b*) – that a given point in space (x_p, y_p) will not necessarily have a unique point with shortest distance to the interface. This is not an issue provided that this system is only required local to the interface so that the normal distance may be assumed to be much less than the radius of curvature. This is acceptable in our situation, where the body-fitted coordinate system is only required to hold in the interface region of $O(Cn)$. Returning to the body-fitted coordinates, we have

$$\boldsymbol{r} = \boldsymbol{r}_0(\zeta^1, t) + \zeta^2 \boldsymbol{n}, \tag{3.10}$$

where $\boldsymbol{n}$ is the unit normal to the interface (noting that $\boldsymbol{n} = \boldsymbol{\nabla} \zeta^2$). The basis vectors are then given by

$$\boldsymbol{e}_1 = (1 - \zeta^2 \kappa)\boldsymbol{t} \quad \text{and} \quad \boldsymbol{e}_2 = \boldsymbol{n}, \tag{3.11}$$

which will be confirmed below, and where $\boldsymbol{t}$ is the unit tangent to the interface and κ is the curvature, so that

$$\boldsymbol{r} = x\boldsymbol{i} + y\boldsymbol{j} = \zeta^1 \boldsymbol{e}_1 + \zeta^2 \boldsymbol{e}_2, \quad \boldsymbol{e}_1 = \frac{\partial x}{\partial \zeta^1}\boldsymbol{i} + \frac{\partial y}{\partial \zeta^1}\boldsymbol{j}, \quad \boldsymbol{e}_2 = \frac{\partial x}{\partial \zeta^2}\boldsymbol{i} + \frac{\partial y}{\partial \zeta^2}\boldsymbol{j}, \tag{3.12}$$

https://doi.org/10.1017/jfm.2013.521 Published online by Cambridge University Press

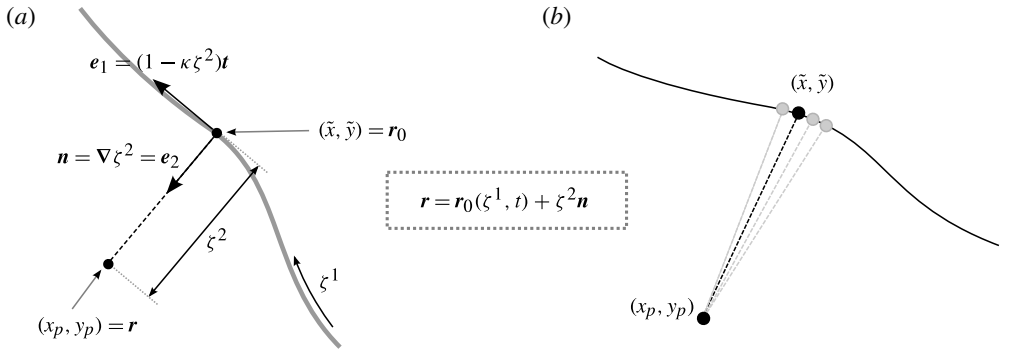


FIGURE 5. (*a*) Schematic of the body-fitted coordinates used to investigate the interfacial region. (*b*) Depiction of the issue of non-uniqueness of points with body-fitted coordinates. Provided the coordinates are only to be used local to the interface (i.e. in the inner region) this problem does not arise, as the normal distance may be assumed to be much less than the radius of curvature.

where $\boldsymbol{i}$ and $\boldsymbol{j}$ are the usual Cartesian basis vectors. We note that $\|\boldsymbol{e}_1\| = \|(1-\zeta^2\kappa)\boldsymbol{t}\| = 1-\zeta^2\kappa$. Next, we let θ be the angle from $\boldsymbol{i}$ to $\boldsymbol{e}_1$, so that the curvature $\kappa = \partial_{\zeta^1}\theta$ (how θ changes as we go along the arclength). At point P on the interface we have X and Y as the specific values of x and y (i.e. at a specific ζ^1). Moving a small amount $\mathrm{d}\zeta^1$ along the interface gives $\mathrm{d}\zeta^1\cos\theta = \mathrm{d}X$ and $\mathrm{d}\zeta^1\sin\theta = \mathrm{d}Y$. Now consider (x, y) to be a point not on the interface, and at a signed distance ζ^2 away. Then we have $x = X - \zeta^2\sin\theta$ and $y = Y + \zeta^2\cos\theta$. Returning to (3.12), we find

$$\boldsymbol{e}_1 = \left(\frac{\partial X}{\partial\zeta^1} - \zeta^2\cos\theta\frac{\partial\theta}{\partial\zeta^1}\right)\boldsymbol{i} + \left(\frac{\partial Y}{\partial\zeta^1} - \zeta^2\sin\theta\frac{\partial\theta}{\partial\zeta^1}\right)\boldsymbol{j} = (1-\kappa\zeta^2)(\cos\theta\boldsymbol{i} + \sin\theta\boldsymbol{j})$$
$$= (1-\kappa\zeta^2)\boldsymbol{t}, \tag{3.13}$$

$$\boldsymbol{e}_2 = \left(\frac{\partial X}{\partial\zeta^2} - \sin\theta\right)\boldsymbol{i} + \left(\frac{\partial Y}{\partial\zeta^2} + \cos\theta\right)\boldsymbol{j} = -\sin\theta\boldsymbol{i} + \cos\theta\boldsymbol{j} = \boldsymbol{n}, \tag{3.14}$$

confirming the above results for the basis vectors. The components of the metric tensor of these curvilinear coordinates are used to determine operators such as the gradient and Laplacian in these coordinates, and are found through $g_{ij} = \boldsymbol{e}_i\cdot\boldsymbol{e}_j$. For orthogonal curvilinear coordinates (such as we have here), where $\{\boldsymbol{e}_1, \boldsymbol{e}_2\}$ and $\{\boldsymbol{e}^1, \boldsymbol{e}^2\}$ are the covariant and contravariant basis vectors respectively, we also have $\boldsymbol{e}^1 = g^{11}\boldsymbol{e}_1 + g^{12}\boldsymbol{e}_2$, $\boldsymbol{e}^2 = g^{12}\boldsymbol{e}_1 + g^{22}\boldsymbol{e}_2$ and $g^{11} = 1/g_{11}$, $g^{22} = 1/g_{22}$, $g^{12} = g_{12} = 0$, so we find

$$g_{11} = (1-\kappa\zeta^2)^2, \quad g_{12} = 0, \quad g_{22} = 1, \tag{3.15a}$$

$$g^{11} = (1-\kappa\zeta^2)^{-2}, \quad g^{12} = 0, \quad g^{22} = 1. \tag{3.15b}$$

We are then able to write down the quantities we require for the governing equations. Time derivatives satisfy

$$\frac{\partial}{\partial t}\phi(x, y, t) = \frac{\partial}{\partial t}\tilde{\phi}(\zeta^1, \zeta^2, t) + \boldsymbol{u}^s\cdot\nabla\tilde{\phi}(\zeta^1, \zeta^2, t), \tag{3.16}$$

where $\boldsymbol{u}^s = (\partial_t\zeta^1, \partial_t\zeta^2)$ is the negative of the interface velocity (chosen in this way for convenience), showing that the time derivative in the comoving frame is a material derivative, and with $\tilde{\phi}$ representing the phase field in inner variables in the body-fitted

https://doi.org/10.1017/jfm.2013.521 Published online by Cambridge University Press

coordinates. Considering $\boldsymbol{u} = (u^1, u^2)$, and writing $h = \sqrt{g_{11}g_{22}}$ for convenience, then

$$\boldsymbol{\nabla}\phi = \frac{\partial\phi}{\partial\zeta^1}\boldsymbol{e}^1 + \frac{\partial\phi}{\partial\zeta^2}\boldsymbol{e}^2 = (1-\kappa\zeta^2)^{-2}\frac{\partial\phi}{\partial\zeta^1}\boldsymbol{e}_1 + \frac{\partial\phi}{\partial\zeta^2}\boldsymbol{e}_2, \tag{3.17}$$

$$|\boldsymbol{\nabla}\phi|^2 = (1-\kappa\zeta^2)^{-2}\left(\frac{\partial\phi}{\partial\zeta^1}\right)^2 + \left(\frac{\partial\phi}{\partial\zeta^2}\right)^2, \tag{3.18}$$

$$\begin{aligned}\boldsymbol{\nabla}\cdot\boldsymbol{u} &= \frac{1}{h}\left[\frac{\partial}{\partial\zeta^1}\left(hu^1\right) + \frac{\partial}{\partial\zeta^2}\left(hu^2\right)\right] \\ &= \frac{\partial u^2}{\partial\zeta^2} - \frac{\kappa u^2}{1-\kappa\zeta^2} + \frac{\partial u^1}{\partial\zeta^1} - \frac{u^1\zeta^2}{1-\kappa\zeta^2}\frac{\partial\kappa}{\partial\zeta^1},\end{aligned} \tag{3.19}$$

$$\begin{aligned}\nabla^2\phi &= \frac{1}{h}\left[\frac{\partial}{\partial\zeta^1}\left(\frac{h}{g_{11}}\frac{\partial\phi}{\partial\zeta^1}\right) + \frac{\partial}{\partial\zeta^2}\left(\frac{h}{g_{22}}\frac{\partial\phi}{\partial\zeta^2}\right)\right] \\ &= \frac{1}{(1-\kappa\zeta^2)^2}\frac{\partial^2\phi}{\partial\zeta^{1^2}} + \frac{\zeta^2}{(1-\kappa\zeta^2)^3}\frac{\partial\kappa}{\partial\zeta^1}\frac{\partial\phi}{\partial\zeta^1} + \frac{\partial^2\phi}{\partial\zeta^{2^2}} - \frac{\kappa}{1-\kappa\zeta^2}\frac{\partial\phi}{\partial\zeta^2}.\end{aligned} \tag{3.20}$$

For certain matrix quantities the Christoffel symbols of the second kind will be required, defined as

$$\Gamma^k_{ij} = \frac{g^{km}}{2}\left(\frac{\partial g_{mi}}{\partial\zeta^j} + \frac{\partial g_{mj}}{\partial\zeta^i} + \frac{\partial g_{ij}}{\partial\zeta^m}\right), \tag{3.21}$$

so that

$$\left.\begin{aligned}\Gamma^1_{11} &= -\frac{\zeta^2}{1-\kappa\zeta^2}\frac{\partial\kappa}{\partial\zeta^1}, \qquad & \Gamma^1_{12} &= \Gamma^1_{21} = -\frac{\kappa}{1-\kappa\zeta^2}, \\ \Gamma^2_{11} &= \frac{\kappa}{1-\kappa\zeta^2}, & \Gamma^k_{ij} &= 0 \text{ otherwise},\end{aligned}\right\} \tag{3.22}$$

which allows us to determine the quantities of interest

$$\boldsymbol{I} = \boldsymbol{e}^1\otimes\boldsymbol{e}_2 + \boldsymbol{e}^2\otimes\boldsymbol{e}_1 = \begin{pmatrix}(1-\kappa\zeta^2)^{-2} & 0\\ 0 & 1\end{pmatrix}, \tag{3.23}$$

$$\boldsymbol{\nabla}\phi\otimes\boldsymbol{\nabla}\phi = \begin{pmatrix}\left[(1-\kappa\zeta^2)^{-2}\dfrac{\partial\phi}{\partial\zeta^1}\right]^2 & \dfrac{1}{(1-\kappa\zeta^2)^2}\dfrac{\partial\phi}{\partial\zeta^1}\dfrac{\partial\phi}{\partial\zeta^2} \\ \dfrac{1}{(1-\kappa\zeta^2)^2}\dfrac{\partial\phi}{\partial\zeta^1}\dfrac{\partial\phi}{\partial\zeta^2} & \left(\dfrac{\partial\phi}{\partial\zeta^2}\right)^2\end{pmatrix}, \tag{3.24}$$

$$\boldsymbol{\nabla}\boldsymbol{u} = \left(\frac{\partial u^i}{\partial\zeta^k} + \Gamma^i_{lk}u^l\right)\boldsymbol{e}_i\otimes\boldsymbol{e}^k, \tag{3.25}$$

where $\boldsymbol{I}$ is the identity tensor, and $\otimes$ represents the dyadic (Kronecker) product, so that

$$(\boldsymbol{\nabla}\boldsymbol{u})^{11} = \frac{\partial u^1}{\partial\zeta^1} - \frac{\partial\kappa}{\partial\zeta^1}\frac{\zeta^2u^1}{1-\kappa\zeta^2} - \frac{\kappa u^2}{1-\kappa\zeta^2}, \quad (\boldsymbol{\nabla}\boldsymbol{u})^{12} = \frac{\partial u^1}{\partial\zeta^2} - \kappa(1-\kappa\zeta^2)u^1, \tag{3.26a}$$

$$(\boldsymbol{\nabla}\boldsymbol{u})^{21} = \frac{\partial u^2}{\partial\zeta^1} + \kappa(1-\kappa\zeta^2)u^1, \quad (\boldsymbol{\nabla}\boldsymbol{u})^{22} = \frac{\partial u^2}{\partial\zeta^2}, \tag{3.26b}$$

https://doi.org/10.1017/jfm.2013.521 Published online by Cambridge University Press

and leads to the components of the viscous stress tensor being

$$\tau^{11} = 2\left(\frac{\partial u^1}{\partial \zeta^1} - \frac{\kappa u^2}{1-\kappa\zeta^2} - \frac{\zeta^2 u^1}{1-\kappa\zeta^2}\frac{\partial \kappa}{\partial \zeta^1}\right), \quad \tau^{12} = \frac{\partial u^1}{\partial \zeta^2} + \frac{\partial u^2}{\partial \zeta^1}, \quad \tau^{22} = 2\frac{\partial u^2}{\partial \zeta^2}, \tag{3.27}$$

with the divergence of a symmetric tensor $\boldsymbol{M}$ satisfying

$$(\boldsymbol{\nabla}\cdot\boldsymbol{M})^1 = \frac{\partial m^{11}}{\partial \zeta^1} + \frac{\partial m^{12}}{\partial \zeta^2} + 2\Gamma^1_{11}m^{11} + 3\Gamma^1_{12}m^{12}, \tag{3.28a}$$

$$(\boldsymbol{\nabla}\cdot\boldsymbol{M})^2 = \frac{\partial m^{12}}{\partial \zeta^1} + \frac{\partial m^{22}}{\partial \zeta^2} + \Gamma^1_{11}m^{12} + \Gamma^1_{12}m^{22} + \Gamma^2_{11}m^{11}. \tag{3.28b}$$

We now transfer to the stretched coordinate $\zeta = \zeta^2/Cn$ to consider the region close to the interface. With this, we have the interface satisfying $\zeta = \zeta^2 = 0$, and we consider the limit $Cn \to 0$ through the expansions

$$\phi = \tilde{\phi}_0 + Cn\,\tilde{\phi}_1 + Cn^2\tilde{\phi}_2 + \cdots, \quad g = \tilde{g}_0 + Cn\,\tilde{g}_1 + Cn^2\tilde{g}_2 + \cdots, \tag{3.29a}$$

$$\boldsymbol{u} = \tilde{\boldsymbol{u}}_0 + Cn\,\tilde{\boldsymbol{u}}_1 + Cn^2\tilde{\boldsymbol{u}}_2 + \cdots, \quad \boldsymbol{\tau} = \frac{1}{Cn}\left[\tilde{\boldsymbol{\tau}}_0 + Cn\,\tilde{\boldsymbol{\tau}}_1 + Cn^2\tilde{\boldsymbol{\tau}}_2 + \cdots\right], \tag{3.29b}$$

$$p = \frac{1}{Cn}\left[\tilde{p}_0 + Cn\,\tilde{p}_1 + Cn^2\tilde{p}_2 + \cdots\right]. \tag{3.29c}$$

3.2.1. *Matching conditions*

At this point we consider the asymptotic matching between inner and outer regions. For an arbitrary function φ, which is $\varphi^\pm$ in the outer region and $\tilde{\varphi}$ in the inner region, we require $\varphi^\pm(\zeta^2) = \varphi^\pm(Cn\,\zeta) \sim \tilde{\varphi}(\zeta)$ for $\zeta \to \infty$, $Cn \to 0$, $\zeta^2 = Cn\,\zeta \to 0$. Thus we have

$$\varphi^\pm(Cn\,\zeta) = \varphi^\pm_0(0) + Cn\left(\zeta\frac{\partial \varphi^\pm_0}{\partial \zeta}(0) + \varphi^\pm_1(0)\right) + \cdots, \quad \tilde{\varphi}(\zeta) = \tilde{\varphi}_0(\zeta) + Cn\tilde{\varphi}_1(\zeta) + \cdots, \tag{3.30}$$

which gives the first two matching conditions at $O(1)$ and $O(Cn)$ as

$$\lim_{\zeta\to\pm\infty}\tilde{\varphi}_0(\zeta) = \varphi^\pm_0(0) \quad \text{and} \quad \lim_{\zeta\to\pm\infty}\tilde{\varphi}_1(\zeta) = \varphi^\pm_1(0) + \zeta\frac{\partial \varphi^\pm_0}{\partial \zeta}(0), \tag{3.31}$$

which imply that

$$\lim_{\zeta\to\pm\infty}\frac{\partial \tilde{\varphi}_1}{\partial \zeta}(\zeta) = \frac{\partial \varphi^\pm_0}{\partial \zeta}(0). \tag{3.32}$$

3.2.2. *Continuity equation*

The continuity equation in body-fitted coordinates (3.19) in inner variables is

$$\frac{1}{Cn}\frac{\partial u^2}{\partial \zeta} - \frac{\kappa u^2}{1-\kappa Cn\,\zeta} + \frac{\partial u^1}{\partial \zeta^1} - Cn\frac{u^1\zeta}{1-\kappa Cn\,\zeta}\frac{\partial \kappa}{\partial \zeta^1} = 0. \tag{3.33}$$

By using the expansions (3.29), the leading order of the continuity equation then satisfies $\partial_\zeta \tilde{u}^2_0 = 0$, and determines that $\tilde{u}^2_0$ is independent of ζ.

https://doi.org/10.1017/jfm.2013.521 Published online by Cambridge University Press

3.2.3. *Cahn–Hilliard type equation*

The Cahn–Hilliard type equation in the inner region gives

$$\frac{\partial \phi}{\partial t} + (\boldsymbol{u}^s + \boldsymbol{u}) \cdot \left[(1 - \kappa Cn\, \zeta)^{-2} \frac{\partial \phi}{\partial \zeta^1} \boldsymbol{e}_1 + \frac{1}{Cn} \frac{\partial \phi}{\partial \zeta} \boldsymbol{e}_2 \right] = \beta \left[\frac{1}{(1 - \kappa Cn\, \zeta)^2} \frac{\partial^2 g}{\partial \zeta^{1 2}} - \frac{1}{Cn} \frac{\kappa}{1 - \kappa Cn\, \zeta} \frac{\partial g}{\partial \zeta} + \frac{Cn\, \zeta}{(1 - \kappa Cn\, \zeta)^3} \frac{\partial \kappa}{\partial \zeta^1} \frac{\partial g}{\partial \zeta^1} + \frac{1}{Cn^2} \frac{\partial^2 g}{\partial \zeta^2} \right], \tag{3.34}$$

so that for the first two orders, using the expansions (3.29) we have

$$\frac{\partial^2 \tilde{g}_0}{\partial \zeta^2} = 0, \quad \frac{\partial \tilde{\phi}_0}{\partial \zeta} (\boldsymbol{u}^s + \tilde{\boldsymbol{u}}_0) \cdot \boldsymbol{e}_2 = \beta \left(\frac{\partial^2 \tilde{g}_1}{\partial \zeta^2} - \kappa \frac{\partial \tilde{g}_0}{\partial \zeta} \right). \tag{3.35}$$

The leading-order equation implies

$$\tilde{g}_0 = \tilde{g}_A(\zeta_1, t)\zeta + \tilde{g}_B(\zeta_1, t), \tag{3.36}$$

and given that, as $\zeta \to \pm\infty$, we need to match to the outer solution, then $\tilde{g}_A = 0$, so that $\tilde{g}_0 = \tilde{g}_B(\zeta_1, t)$, i.e. $\tilde{g}_0$ is independent of ζ.

To be more precise about this point, we know that in the outer region we require $g^{\pm} \to 0$ away from the interface. If $\tilde{g}_0 = \tilde{g}_A(\zeta^1, t)\zeta + \tilde{g}_B(\zeta^1, t)$, then for $\tilde{g}_A(\zeta^1, t) \neq 0$, $\tilde{g}_0 \sim \tilde{g}_A(\zeta^1, t)\zeta$ as $\zeta \to \pm\infty$ to match. Thus for this to be the matching behaviour to the bulk fluids on both sides of the interface, and for the chemical potential to vanish far from the interface (in the outer region), then there would have to be a turning point in the chemical potential away from the boundaries in one of the outer regions, unless $\tilde{g}_A(\zeta^1, t) = 0$. A turning point is, however, excluded by the maximum principle as the leading-order chemical potential is harmonic in the outer regions, thus we must have $\tilde{g}_A = 0$, so that $\tilde{g}_0 = \tilde{g}_B(\zeta^1, t)$.

The next order thus gives

$$(\tilde{u}_n^s + \tilde{u}_0^2) \frac{\partial \tilde{\phi}_0}{\partial \zeta} = \beta \frac{\partial^2 \tilde{g}_1}{\partial \zeta^2}. \tag{3.37}$$

We already know that $\tilde{u}_0^2$ is independent of the normal coordinate ζ, and as the normal interface velocity is also independent of ζ, integrating gives

$$\left[(\tilde{u}_n^s + \tilde{u}_0^2) \tilde{\phi}_0 \right]_{-\infty}^{\infty} = \beta \left[\frac{\partial \tilde{g}_1}{\partial \zeta} \right]_{-\infty}^{\infty}, \tag{3.38}$$

implying

$$2(u_n^s + u_0^{2\pm}) = \beta \left[\frac{\partial g_0^+}{\partial \zeta}(0) - \frac{\partial g_0^-}{\partial \zeta}(0) \right]. \tag{3.39}$$

This equation tells us how the interface moves. If the gradients in the chemical potential differ on either side of the interface, then the interface translates both by advection and through diffusion of matter. This diffusion would be non-classical and is sometimes termed spurious diffusion, for example in related studies by Swift *et al.* (1996) and Le Roy *et al.* (2010). If the chemical potential gradients cancel, then the diffusion of matter in and out balance and the interface moves through advection alone. We will see in the next section that changing the constant mobility to one with phase field dependence can guarantee that no spurious diffusion can occur at this order in

https://doi.org/10.1017/jfm.2013.521 Published online by Cambridge University Press

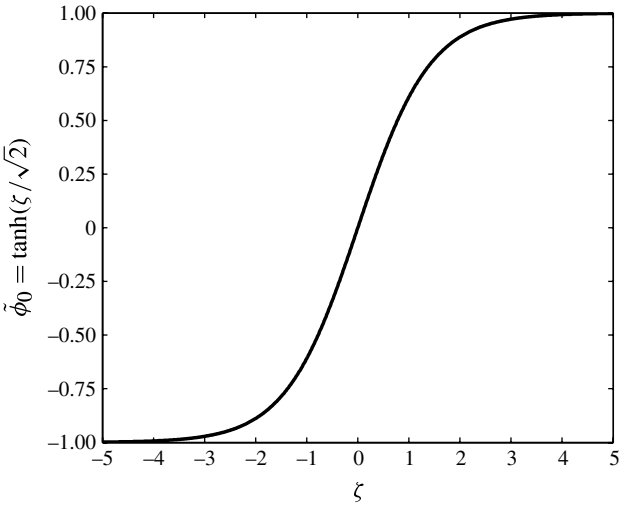


FIGURE 6. The profile of the leading-order solution of the phase field in the inner region.

the sharp-interface limit, as the terms involving the chemical potential gradient do not appear. However, for the current model we can merely say that if these terms balance we recover the classical hydrodynamic model, and thus $u_n^s = -u_0^{2\pm}$, the normal velocity of the interface is equal to the normal velocity of the fluids (and negative due to the way we have defined it). This would then also be equivalent to the expression

$$\frac{\partial \zeta^2}{\partial t} + \boldsymbol{u}_0^{\pm} \cdot \nabla \zeta^2 = 0, \tag{3.40}$$

the expected kinematic boundary condition for the sharp interface defined by $\zeta^2 = 0$.

3.2.4. *Chemical potential equation*

We now consider the chemical potential equation in the inner region

$$\frac{4Cn}{3\sqrt{2}} g = (\phi^2 - 1)\phi - \frac{Cn^2}{(1 - \kappa Cn\,\zeta)^2} \frac{\partial^2 \phi}{\partial {\zeta^1}^2} - \frac{\partial^2 \phi}{\partial \zeta^2} - \frac{Cn^3 \zeta (\partial_{\zeta^1} \kappa)}{(1 - \kappa Cn\,\zeta)^3} \frac{\partial \phi}{\partial \zeta^1} + \frac{Cn\kappa}{1 - \kappa Cn\,\zeta} \frac{\partial \phi}{\partial \zeta}, \tag{3.41}$$

so that using the expansions (3.29), we have at leading order

$$-\frac{\partial^2 \tilde{\phi}_0}{\partial \zeta^2} + \tilde{\phi}_0(\tilde{\phi}_0^2 - 1) = 0, \tag{3.42}$$

with the solution corresponding to the matching conditions $\tilde{\phi}_0 \to \pm 1$ and $\partial_\zeta \tilde{\phi}_0 \to 0$ as $\zeta \to \pm\infty$, and $\tilde{\phi}_0|_{\zeta=0} = 0$ being

$$\tilde{\phi}_0 = \tanh\left(\frac{\zeta}{\sqrt{2}}\right), \tag{3.43}$$

which is shown in figure 6, and we note that $\tilde{\phi}_0 = \tilde{\phi}_0(\zeta)$, i.e. it is independent of ζ^1. More details on obtaining this solution and discussion on a general solution relevant to other boundary conditions may be found in appendix B.1.

https://doi.org/10.1017/jfm.2013.521 Published online by Cambridge University Press

At the next order in the chemical potential equation we find

$$\tilde{g}_0 = \frac{3\sqrt{2}}{4}\left\{\tilde{\phi}_1(3\tilde{\phi}_0^2 - 1) - \left(\frac{\partial^2\tilde{\phi}_1}{\partial\zeta^2} - \kappa\frac{\partial\tilde{\phi}_0}{\partial\zeta}\right)\right\}. \tag{3.44}$$

We consider the above equation in the limit as the outer region is approached, and will then follow the usual approach of finding a solvability condition for the above equation afterwards. We can see from (3.43) that $\lim_{\zeta\to\pm\infty}\partial_\zeta\tilde{\phi}_0 = 0$, and that $\lim_{\zeta\to\pm\infty}(3\tilde{\phi}_0^2 - 1) = 2$, so that

$$\frac{4}{3\sqrt{2}}\lim_{\zeta\to\pm\infty}\tilde{g}_0 = 2\lim_{\zeta\to\pm\infty}\tilde{\phi}_1 - \lim_{\zeta\to\pm\infty}\frac{\partial^2\tilde{\phi}_1}{\partial\zeta^2}, \tag{3.45}$$

and since $\lim_{\zeta\to\pm\infty}\tilde{\phi}_1 = \phi_1^{\pm}(0) + \zeta\,\partial_\zeta\phi_0^{\pm}(0) = \phi_1^{\pm}(0)$, and that $\tilde{g}_0 = \tilde{g}_B(\zeta^1, t)$ from the leading-order Cahn–Hilliard type equation, then we are left with

$$\frac{4}{3\sqrt{2}}\tilde{g}_B + \lim_{\zeta\to\pm\infty}\frac{\partial^2\tilde{\phi}_1}{\partial\zeta^2} = 2\phi_1^{\pm}(0). \tag{3.46}$$

Consider $\eta = 1/\zeta$, so that $\partial_\zeta = -\eta^2\partial_\eta$. Thus

$$-\frac{\partial^2\tilde{\phi}_1}{\partial\zeta^2} = -\frac{\partial}{\partial\zeta}\left(-\eta^2\frac{\partial\tilde{\phi}_1}{\partial\eta}\right) = -\eta^2\frac{\partial}{\partial\eta}\left(\eta^2\frac{\partial\tilde{\phi}_1}{\partial\eta}\right) = -\eta^2\left(2\eta\frac{\partial\tilde{\phi}_1}{\partial\eta} + \eta^2\frac{\partial^2\tilde{\phi}_1}{\partial\eta^2}\right). \tag{3.47}$$

Now as $\zeta\to\infty$ we have $\eta\to 0$, thus using (3.46) and assuming $\tilde{\phi}_1 \sim A_1\eta^m$, it follows that

$$\frac{4}{3\sqrt{2}}\tilde{g}_B \sim \lim_{\eta\to 0}\left[2A_1\eta^m - A_1 m(m+1)\eta^{m+2}\right]. \tag{3.48}$$

In the surface diffusion case considered by Gugenberger *et al.* (2008), the authors obtain the result that $\phi_1^{\pm} = 0$ so that the $2\lim_{\eta\to 0}(A_1\eta^m)$ term is not present. This crucially allows them to balance the remaining terms to find $m = -2$ and thus $-(\sqrt{2}/3)\tilde{g}_B = A_1$, which means that $\tilde{\phi}_1 \sim -(\sqrt{2}/3)\tilde{g}_B\zeta^2$ is divergent, and thus $\tilde{g}_B = 0$ to match to the outer solution. Here the result is not as strong, but we saw that non-classical terms arise at next to leading order in the bulk fluid regions unless $g_0^{\pm} = \phi_1^{\pm} = 0$, i.e. unless $\tilde{g}_B = 0$, through matching. We continue in the general situation where $\tilde{g}_B$ remains undetermined.

The usual sharp-interface limit considerations miss this point, and search for a solvability condition motivated by the Fredholm alternative. For detailed use of the Fredholm alternative see appendix B.2, but here we take a common approach that circumvents the technical details by multiplying (3.44) with $\partial_\zeta\tilde{\phi}_0$ and integrating

$$\int_{-\infty}^{\infty}\left[-\frac{\partial^2\tilde{\phi}_1}{\partial\zeta^2} + \tilde{\phi}_1(3\tilde{\phi}_0^2 - 1)\right]\frac{\partial\tilde{\phi}_0}{\partial\zeta}\,\mathrm{d}\zeta = -\left[\frac{\partial\tilde{\phi}_0}{\partial\zeta}\frac{\partial\tilde{\phi}_1}{\partial\zeta} - \frac{\partial^2\tilde{\phi}_0}{\partial\zeta^2}\tilde{\phi}_1\right]_{-\infty}^{\infty} = 0, \tag{3.49}$$

found via multiple integration by parts, which then implies the solvability condition

$$\int_{-\infty}^{\infty}\left[\frac{2\sqrt{2}}{3}\tilde{g}_B - \kappa\frac{\partial\tilde{\phi}_0}{\partial\zeta}\right]\frac{\partial\tilde{\phi}_0}{\partial\zeta}\,\mathrm{d}\zeta = 0, \tag{3.50}$$

https://doi.org/10.1017/jfm.2013.521 Published online by Cambridge University Press

and which determines

$$\frac{4\sqrt{2}}{3}\tilde{g}_B - \kappa\int_{-\infty}^{\infty}\left[\frac{\partial\tilde{\phi}_0}{\partial\zeta}\right]^2 \mathrm{d}\zeta = 0, \quad \Rightarrow 2\tilde{g}_B = \kappa. \tag{3.51}$$

This result is obtained by using the result (3.43), which gives

$$\int_{-\infty}^{\infty}\left(\frac{\partial\tilde{\phi}_0}{\partial\zeta}\right)^2 \mathrm{d}\zeta = \frac{1}{2}\int_{-\infty}^{\infty}\mathrm{sech}^4\left(\frac{\zeta}{\sqrt{2}}\right)\mathrm{d}\zeta = \frac{2\sqrt{2}}{3}. \tag{3.52}$$

We obtain that $2\tilde{g}_B = \kappa$, and if only classical terms in the bulk fluids to at least next to leading order in the sharp-interface limit are required, then $\tilde{g}_B = 0$, and hence the curvature of the interface $\kappa = 0$, i.e. to this order the interface would be flat.

3.2.5. *Momentum equation*

We next consider the momentum equation in the body-fitted coordinates,

$$\begin{aligned} Re\left(\frac{\partial\boldsymbol{u}}{\partial t} + (\boldsymbol{u}^s + \boldsymbol{u})\cdot\boldsymbol{\nabla}\boldsymbol{u}\right) = &-\left((1-\kappa\zeta^2)^{-2}\frac{\partial p}{\partial\zeta^1}\boldsymbol{e}_1 + \frac{\partial p}{\partial\zeta^2}\boldsymbol{e}_2\right) \\ &+\begin{pmatrix} \dfrac{\partial\tau^{11}}{\partial\zeta^1} + \dfrac{\partial\tau^{12}}{\partial\zeta^2} + 2\Gamma^1_{11}\tau^{11} + 3\Gamma^1_{12}\tau^{12} \\ \dfrac{\partial\tau^{12}}{\partial\zeta^1} + \dfrac{\partial\tau^{22}}{\partial\zeta^2} + \Gamma^1_{11}\tau^{12} + \Gamma^1_{12}\tau^{22} + \Gamma^2_{11}\tau^{11} \end{pmatrix} \\ &+\frac{1}{Ca}g\left((1-\kappa\zeta^2)^{-2}\frac{\partial\phi}{\partial\zeta^1}\boldsymbol{e}_1 + \frac{\partial\phi}{\partial\zeta^2}\boldsymbol{e}_2\right), \end{aligned} \tag{3.53}$$

where the components of $\boldsymbol{\nabla}\boldsymbol{u}$ are given in (3.26), the Christoffel symbols Γ^k_{ij} in (3.22), and the viscous stress components in (3.27). At leading order in the inner region we have

$$\frac{\partial\tilde{\tau}_0^{12}}{\partial\zeta} = 0, \quad \frac{\partial}{\partial\zeta}(-\tilde{p}_0 + \tilde{\tau}_0^{22}) = 0 \tag{3.54}$$

(where $\tilde{\tau}_0^{12} = \partial_\zeta\tilde{u}_0^1$ and $\tilde{\tau}_0^{22} = 2\partial_\zeta\tilde{u}_0^2$), and integrating once suggests that these leading-order stress components are independent of ζ. Applying the matching conditions we find that $\lim_{\zeta\to\pm\infty}\tilde{\boldsymbol{\tau}}_0 = 0$, and $\lim_{\zeta\to\pm\infty}\tilde{p}_0 = 0$ thus $\tilde{\tau}_0^{12} = 0$ and $\tilde{\tau}_0^{22} = \tilde{p}_0$, which gives the result that $\tilde{u}_0^1$ is independent of ζ. As we already know that $\tilde{u}_0^2$ is independent of ζ from the continuity equation, we thus have the interface condition $\tilde{\boldsymbol{u}}_0^+ = \tilde{\boldsymbol{u}}_0^-$, and find that $\tilde{p}_0 = 0$. The next order in the momentum equation then suggests

$$\begin{aligned} Re(\boldsymbol{u}^s + \tilde{\boldsymbol{u}}_0)\cdot\begin{pmatrix} 0 & \dfrac{\partial\tilde{u}_0^1}{\partial\zeta} \\ 0 & \dfrac{\partial\tilde{u}_0^2}{\partial\zeta} \end{pmatrix} = &-\begin{pmatrix} \dfrac{\partial\tilde{p}_0}{\partial\zeta^1} \\ \dfrac{\partial\tilde{p}_1}{\partial\zeta} \end{pmatrix} + \begin{pmatrix} \dfrac{\partial\tilde{\tau}_0^{11}}{\partial\zeta^1} + \dfrac{\partial\tilde{\tau}_1^{12}}{\partial\zeta} - 3\kappa\tilde{\tau}_0^{12} \\ \dfrac{\partial\tilde{\tau}_0^{12}}{\partial\zeta^1} + \dfrac{\partial\tilde{\tau}_1^{22}}{\partial\zeta} + \kappa(\tilde{\tau}_0^{11} - \tilde{\tau}_0^{22}) \end{pmatrix} \\ &+\frac{\tilde{g}_0}{Ca}\frac{\partial\tilde{\phi}_0}{\partial\zeta}\boldsymbol{e}_2, \end{aligned} \tag{3.55}$$

and on using results found from the leading-order solution, these reduce to

$$\frac{\partial\tilde{\tau}_0^{11}}{\partial\zeta^1} + \frac{\partial\tilde{\tau}_1^{12}}{\partial\zeta} = 0, \quad -\frac{\partial\tilde{p}_1}{\partial\zeta} + \frac{\partial\tilde{\tau}_1^{22}}{\partial\zeta} + \kappa\tilde{\tau}_0^{11} + \frac{\tilde{g}_0}{Ca}\frac{\partial\tilde{\phi}_0}{\partial\zeta} = 0. \tag{3.56}$$

https://doi.org/10.1017/jfm.2013.521 Published online by Cambridge University Press

Now $\tilde{\tau}_0^{11} = 0$ (from its definition), and substituting for the other stresses, we have

$$\frac{\partial}{\partial \zeta}\left(\frac{\partial \tilde{u}_1^1}{\partial \zeta} + \frac{\partial \tilde{u}_0^2}{\partial \zeta^1}\right) = 0, \quad -\frac{\partial \tilde{p}_1}{\partial \zeta} + 2\frac{\partial^2 \tilde{u}_1^2}{\partial \zeta^2} + \frac{\tilde{g}_0}{Ca}\frac{\partial \tilde{\phi}_0}{\partial \zeta} = 0. \tag{3.57}$$

It is more convenient to write these equations as

$$\frac{\partial \tilde{\tau}_1^{12}}{\partial \zeta} = 0, \quad \frac{\partial \tilde{\tau}_1^{22}}{\partial \zeta} = \frac{\partial \tilde{p}_1}{\partial \zeta} - \frac{\tilde{g}_0}{Ca}\frac{\partial \tilde{\phi}_0}{\partial \zeta}. \tag{3.58}$$

Integrating the next-order momentum equations yields

$$\left[\tilde{\tau}_1^{12}\right]_{-\infty}^{\infty} = 0, \quad \left[\tilde{\tau}_1^{22}\right]_{-\infty}^{\infty} = \left[\tilde{p}_1\right]_{-\infty}^{\infty} - \frac{2\tilde{g}_B}{Ca}, \tag{3.59}$$

and matching to the outer region gives the interface conditions

$$\boldsymbol{n} \cdot [\boldsymbol{\tau}_0^+ - \boldsymbol{\tau}_0^-] \cdot (\boldsymbol{I} - \boldsymbol{n} \otimes \boldsymbol{n}) = 0, \tag{3.60a}$$

$$\boldsymbol{n} \cdot [(-p_0^+ + p_0^-)\boldsymbol{I} + \boldsymbol{\tau}_0^+ - \boldsymbol{\tau}_0^-] \cdot \boldsymbol{n} = -\frac{2\tilde{g}_B}{Ca} = -\frac{\kappa}{Ca}. \tag{3.60b}$$

For unknown $g_0^{\pm}$ in the outer region, these boundary conditions are the classical tangential and normal stress balances. However, $g_0^{\pm} \neq 0$ in this instance, since $\tilde{g}_B = \kappa/2 \neq 0$, and these must match, so there are non-classical terms in the outer region at $O(Cn)$ in the sharp-interface limit. If $g_0^{\pm} = 0$, then $\kappa = 0$ and these conditions are only correct at equilibrium. In § 8 we will consider a modification to the mobility which overcomes this limitation.

4. Phase field dependent mobility

4.1. *Governing equations with phase field dependent mobility*

The dimensional governing equations when the mobility is phase field dependent are again given by (2.2)–(2.6), but here we consider $\gamma = M_1\gamma_1 = M_1(1-\phi^2)$, or $\gamma = M_2\gamma_2 = M_2(1-\phi^2)^2$. These may be non-dimensionalized with (2.10), and contain the same non-dimensional parameters, but with $\beta = M_i\sigma/L^2U$ for $i = \{1, 2\}$ slightly modified from its previous representation. The equations become (2.12)–(2.14), but with the Cahn–Hilliard type equation modified to

$$\frac{\partial \phi}{\partial t} + \boldsymbol{u} \cdot \nabla\phi = \beta \nabla \cdot (\gamma_i \nabla g)\,, \tag{4.1}$$

where γ_i is for $i = \{1, 2\}$, with $\gamma_1 = 1 - \phi^2$ and $\gamma_2 = (1-\phi^2)^2$. The form of γ_1 is used in the droplet dewetting and pinch-off study of Jiang *et al.* (2012), but clearly other possibilities exist; as such we also demonstrate the asymptotics for another form γ_2, the analogue of a form used by Yeon, Cha & Grant (2006), albeit for a very different model and application. These equations may be formed by choosing $\alpha = 0$, $\mathscr{B} = 0$, and $\mathscr{C} = 1$ in the combined equation system of figure 2.

4.2. *The outer region*

In the outer region for the bulk fluids away from the interface we again take the expansions (3.1) along with $\gamma_i = \gamma_{i0}^{\pm} + Cn\gamma_{i1}^{\pm} + \cdots$, and find $\phi_0^{\pm} = \pm 1$ at leading order along with the Navier–Stokes equations as in (3.2)–(3.3), and

$$\nabla \cdot \left(\gamma_{i0}^{\pm} \nabla g_0^{\pm}\right) = 0, \tag{4.2}$$

https://doi.org/10.1017/jfm.2013.521 Published online by Cambridge University Press

where $\gamma_{i0}^{\pm}$ represents $\gamma_{10}^{\pm} = 1 - \phi_0^{\pm 2}$ or $\gamma_{20}^{\pm} = (1 - \phi_0^{\pm 2})^2$, so that $\gamma_{i0}^{\pm} = 0$ and (4.2) is automatically satisfied. The following order gives (3.5)–(3.6) and

$$\frac{\partial \phi_1^{\pm}}{\partial t} + \boldsymbol{u}_0^{\pm} \cdot \boldsymbol{\nabla} \phi_1^{\pm} = \beta \boldsymbol{\nabla} \cdot \left(\gamma_{i1}^{\pm} \boldsymbol{\nabla} g_0^{\pm} \right), \quad g_0^{\pm} = \frac{3\sqrt{2}}{2} \phi_1^{\pm}, \tag{4.3}$$

having used that $\phi_0^{\pm} = \pm 1$ and $\gamma_{i0}^{\pm} = 0$ to remove some terms already. Now $\gamma_{i1}^{\pm}$ stands for $\gamma_{01}^{\pm} = -2\phi_0^{\pm}\phi_1^{\pm}$ and $\gamma_{11}^{\pm} = -4(1 - \phi_0^{\pm 2})\phi_0^{\pm}\phi_1^{\pm}$. Once again, non-classical terms enter at this order, and to exclude them we would require $g_0^{\pm} = \phi_1^{\pm} = 0$.

4.3. *The inner region*

The process is the same as before, so we go straight to the equations, and obtain the same result from the continuity equation, i.e. that $\tilde{u}_0^2$ is independent of ζ. The Cahn–Hilliard type equation in body-fitted coordinates in the inner region is

$$\begin{aligned} &\frac{\partial \phi}{\partial t} + (\boldsymbol{u}^s + \boldsymbol{u}) \cdot \left[(1 - \kappa Cn\, \zeta)^{-2} \frac{\partial \phi}{\partial \zeta^1} \boldsymbol{e}_1 + \frac{1}{Cn} \frac{\partial \phi}{\partial \zeta} \boldsymbol{e}_2 \right] \\ &\quad = \beta \left\{ \frac{1}{Cn} \frac{\partial \lambda_2}{\partial \zeta} - \frac{\kappa \lambda_2}{1 - \kappa Cn\, \zeta} + \frac{\partial \lambda_1}{\partial \zeta^1} - \frac{Cn \lambda_1 \zeta}{1 - \kappa Cn\, \zeta} \frac{\partial \kappa}{\partial \zeta^1} \right\}, \end{aligned} \tag{4.4}$$

$$\lambda_1 = \gamma_i (1 - \kappa Cn\, \zeta)^{-2} \frac{\partial g}{\partial \zeta^1}, \quad \lambda_2 = \gamma_i \frac{1}{Cn} \frac{\partial g}{\partial \zeta}, \tag{4.5}$$

so that for the first two orders, using the expansions (3.29) we have

$$\frac{\partial}{\partial \zeta} \left(\tilde{\gamma}_{i0} \frac{\partial \tilde{g}_0}{\partial \zeta} \right) = 0, \quad \tilde{\gamma}_{10} = 1 - \tilde{\phi}_0^2, \quad \tilde{\gamma}_{20} = (1 - \tilde{\phi}_0^2)^2, \tag{4.6a}$$

$$\frac{\partial \tilde{\phi}_0}{\partial \zeta} (\boldsymbol{u}^s + \tilde{\boldsymbol{u}}_0) \cdot \boldsymbol{e}_2 = \beta \left[\frac{\partial}{\partial \zeta} \left(\tilde{\gamma}_{i0} \frac{\partial \tilde{g}_1}{\partial \zeta} + \tilde{\gamma}_{i1} \frac{\partial \tilde{g}_0}{\partial \zeta} \right) - \kappa \tilde{\gamma}_{i0} \frac{\partial \tilde{g}_0}{\partial \zeta} \right]. \tag{4.6b}$$

The leading-order equation implies $\tilde{\gamma}_{i0} \partial_\zeta \tilde{g}_0 = \tilde{g}_A(\zeta_1, t)$, and given that as $\zeta \to \pm\infty$, we need to match to the outer solution, then $\tilde{g}_A = 0$, since $\tilde{\gamma}_{i0} \to 0$. We will see later that the solution from the chemical potential equation for $\tilde{\phi}_0$ does not then give $\tilde{\gamma}_{i0} = 0$ in the inner region, and hence $\partial_\zeta \tilde{g}_0 = 0$, thus $\tilde{g}_0 = \tilde{g}_B(\zeta_1, t)$, i.e. $\tilde{g}_0$ is independent of ζ.

The next order thus gives

$$(\tilde{u}_n^s + \tilde{u}_0^2) \frac{\partial \tilde{\phi}_0}{\partial \zeta} = \beta \frac{\partial}{\partial \zeta} \left(\tilde{\gamma}_{i0} \frac{\partial \tilde{g}_1}{\partial \zeta} \right). \tag{4.7}$$

We already know that $\tilde{u}_0^2$ is independent of ζ, so assuming that the normal interface velocity is also independent of the normal coordinate ζ, then integrating gives

$$\left[(\tilde{u}_n^s + \tilde{u}_0^2) \tilde{\phi}_0 \right]_{-\infty}^{\infty} = \beta \left[\tilde{\gamma}_{i0} \frac{\partial \tilde{g}_1}{\partial \zeta} \right]_{-\infty}^{\infty}, \tag{4.8}$$

implying

$$2(u_n^s + u_0^{2\pm}) = 0, \tag{4.9}$$

so that $u_n^s = -u_0^{2\pm}$. In the case of phase field dependent mobility, then, there is no possibility of having spurious diffusion at this order in the sharp-interface limit, as the mobility forms prevent leading-order diffusion in the bulk, with $\tilde{\gamma}_{i0} \to 0$ as $\zeta \to \pm\infty$. Instead, we are guaranteed the classical kinematic boundary condition (3.40) for the sharp interface defined by $\zeta^2 = 0$.

https://doi.org/10.1017/jfm.2013.521 Published online by Cambridge University Press

The analysis of the chemical potential and momentum equations will follow as for the original CH case, and as such

$$\tilde{\phi}_0 = \tanh\left(\frac{\zeta}{\sqrt{2}}\right), \quad \tilde{g}_0 = \tilde{g}_B = \frac{3\sqrt{2}}{4}\left\{\tilde{\phi}_1(3\tilde{\phi}_0^2 - 1) - \left(\frac{\partial^2\tilde{\phi}_1}{\partial\zeta^2} - \kappa\frac{\partial\tilde{\phi}_0}{\partial\zeta}\right)\right\}, \tag{4.10}$$

$$\tilde{\tau}_0^{11} = \tilde{\tau}_0^{12} = \tilde{\tau}_0^{22} = \tilde{p}_0 = 0, \quad \tilde{\boldsymbol{u}}_0^+ = \tilde{\boldsymbol{u}}_0^-, \quad \frac{\partial\tilde{\tau}_1^{12}}{\partial\zeta} = 0, \quad \frac{\partial\tilde{\tau}_1^{22}}{\partial\zeta} = \frac{\partial\tilde{p}_1}{\partial\zeta} - \frac{\tilde{g}_B}{Ca}\frac{\partial\tilde{\phi}_0}{\partial\zeta}. \tag{4.11}$$

The solvability condition for $\tilde{\phi}_1$ from (4.10) once again determines $2\tilde{g}_B = \kappa$, and results from the momentum equations (4.11) give

$$\boldsymbol{n}\cdot[\boldsymbol{\tau}_0^+ - \boldsymbol{\tau}_0^-]\cdot(\boldsymbol{I} - \boldsymbol{n}\otimes\boldsymbol{n}) = 0, \tag{4.12a}$$

$$\boldsymbol{n}\cdot[(-p_0^+ + p_0^-)\boldsymbol{I} + \boldsymbol{\tau}_0^+ - \boldsymbol{\tau}_0^-]\cdot\boldsymbol{n} = -\frac{2\tilde{g}_B}{Ca}. \tag{4.12b}$$

In the same way as for the original CH model, the result $2\tilde{g}_B = \kappa$ forces $\kappa = 0$ if next to leading-order outer equations are to be formed of classical terms only, and thus the correct boundary conditions in the sharp-interface limit will only be recovered at equilibrium.

5. Non-conservative model

Thus far we have looked at conservative models based on the Cahn–Hilliard equation (Cahn & Hilliard 1958). Non-conservative models have also been considered in the literature, being based on the Allen–Cahn equation (Allen & Cahn 1979), such as the work by Biben *et al.* (2003) in which drop dynamics are modelled in an external flow, and by Yang *et al.* (2006) on jet pinch-off and drop formation.

The purpose of this section is to show that a model similar to the CH model of § 3, but with a non-conservative Allen–Cahn form, rather than conservative Cahn–Hilliard form, can improve on the feature of having non-classical terms at next to leading order in the bulk equations. Such a hypothetical model will not conserve the volume fractions of the liquids, and hence is not a good choice of model for immiscible two-phase flow, but will provide motivation to consider more complex conserved models in the later sections.

Before proceeding with the analysis of this hypothetical model, we note that the models cited above, used by Biben *et al.* (2003) and Yang *et al.* (2006), have additional terms to either force volume fraction conservation or to alleviate other issues, e.g. to cancel a non-physical relaxation due to a surface tension that is not coupled to the velocity field. They also have subtly different stresses in their respective momentum equations (to each other, and to the CH model). The focus of the present work is to compare a number of binary fluid models based on coupled Cahn–Hilliard/Navier–Stokes equations, which automatically conserve volume fractions without needing to force this separately (for example through a numerically calculated Lagrange multiplier, as in Yang *et al.* 2006). A detailed sharp-interface analysis of a model closely related (and inspiring) that of Biben *et al.* (2003) is given by Folch *et al.* (1999), for the interested reader.

Returning to our hypothetical non-conserved model, the dimensional form we will consider here was introduced in (2.7), and given in non-dimensional form in (2.16). The system of equations to consider are thus (2.12)–(2.14), with the Allen–Cahn type

https://doi.org/10.1017/jfm.2013.521 Published online by Cambridge University Press

equation (2.16), formed by choosing $\beta = 0$, $\mathscr{B} = 0$, and $\mathscr{C} = 1$ in the combined equation system of figure 2.

5.1. *The outer region*

In the outer region for the bulk fluids away from the interface we take $Cn \to 0$ and use the expansions in (3.1). At leading order we find that $\phi_0^\pm = \pm 1$, and the Navier–Stokes equations as in (3.2)–(3.4), but with the Allen–Cahn type equation significantly now forcing $g_0^\pm = 0$. The following order gives the linearized Navier–Stokes equations

$$\boldsymbol{\nabla} \cdot \boldsymbol{u}_1^\pm = 0, \quad Re\left(\frac{\partial \boldsymbol{u}_1^\pm}{\partial t} + \boldsymbol{u}_0^\pm \cdot \boldsymbol{\nabla}\boldsymbol{u}_1^\pm + \boldsymbol{u}_1^\pm \cdot \boldsymbol{\nabla}\boldsymbol{u}_0^\pm\right) = -\boldsymbol{\nabla} p_1^\pm + \nabla^2 \boldsymbol{u}_1^\pm, \tag{5.1}$$

differing from the conserved model CH since no non-classical terms enter, and the remaining equations give

$$\frac{\partial \phi_1^\pm}{\partial t} + \boldsymbol{u}_0^\pm \cdot \boldsymbol{\nabla}\phi_1^\pm = -\alpha g_1^\pm, \quad 0 = g_0^\pm = \frac{3\sqrt{2}}{4}\phi_1^\pm(3\phi_0^{\pm 2} - 1) = \frac{3\sqrt{2}}{2}\phi_1^\pm, \tag{5.2}$$

having used that $g_0^\pm = 0$ and $\phi_0^\pm = \pm 1$ to remove some terms already.

In general in this case, we can see that

$$\phi(t, x, y) = \phi_0^\pm + 0 + \cdots + Cn^j \phi_j^\pm + \cdots, \quad g(t, x, y) = Cn^{j-1} g_{j-1}^\pm + \cdots, \tag{5.3}$$

so that

$$g_{j-1}^\pm = \frac{3\sqrt{2}}{4}\left[(3\phi_0^{\pm 2} - 1)\phi_j^\pm - \nabla^2 \phi_{j-2}^\pm\right] = \frac{3\sqrt{2}}{2}\phi_j^\pm \quad \text{and} \quad -g_{j-1}^\pm = 0, \tag{5.4}$$

and thus $\phi_j^\pm = 0$. As such, in the outer region we have that

$$g = g^\pm = 0 \quad \text{and} \quad \phi = \phi^\pm = \pm 1, \tag{5.5}$$

to all orders in Cn, with linearized versions of the incompressible Navier–Stokes equations being satisfied by the fluid velocity and pressure.

5.2. *The inner region*

The process is the same as before, using expansions (3.29) and matching conditions from § 3.2.1. The continuity equation follows as for the CH model case, finding that $\tilde{u}_0^2$ is independent of ζ.

5.2.1. *Allen–Cahn type equation*

The Allen–Cahn type equation in body-fitted coordinates and in the inner regions gives

$$\frac{\partial \phi}{\partial t} + (\boldsymbol{u}^s + \boldsymbol{u}) \cdot \left[\frac{\dfrac{\partial \phi}{\partial \zeta^1}}{(1 - \kappa Cn\, \zeta)^2}\boldsymbol{e}_1 + \frac{1}{Cn}\frac{\partial \phi}{\partial \zeta}\boldsymbol{e}_2\right] = -\alpha g, \tag{5.6}$$

so that for the first two orders, using the expansions (3.29) we have

$$\frac{\partial \tilde{\phi}_0}{\partial \zeta}(\boldsymbol{u}^s + \tilde{\boldsymbol{u}}_0) \cdot \boldsymbol{e}_2 = 0 \quad \text{and} \quad (\boldsymbol{u}^s + \tilde{\boldsymbol{u}}_0) \cdot \left[\frac{\partial \tilde{\phi}_1}{\partial \zeta}\boldsymbol{e}_2\right] + \frac{\partial \tilde{\phi}_0}{\partial \zeta}\tilde{\boldsymbol{u}}_1 \cdot \boldsymbol{e}_2 = -\alpha \tilde{g}_0, \tag{5.7}$$

https://doi.org/10.1017/jfm.2013.521 Published online by Cambridge University Press

where the time and ζ^1 derivative terms of $\tilde{\phi}_0$ are cancelled, as we will find that $\tilde{\phi}_0 = \tilde{\phi}_0(\zeta)$ as in the previous cases. The leading-order equation suggests that

$$u_n^s + u_0^{2\pm} = 0, \tag{5.8}$$

as we will see that $\partial_\zeta \tilde{\phi}_0 \neq 0$. Thus the condition becomes $u_n^s = -u_0^{2\pm}$, and the normal velocity of the interface is equal to the normal velocity of the fluids and recovers the expected kinematic boundary condition (3.40) for the sharp interface defined by $\zeta^2 = 0$. We also note that here there can be no spurious diffusion for this non-conserved form, even with a constant 'mobility' α, unlike the CH model, which did not prevent this at the equivalent order in the sharp-interface limit.

5.2.2. *Chemical potential equation*

The chemical potential equation in the inner region is the same as for the original conserved model: at leading order the same solution (3.43) is found, where $\tilde{\phi}_0 = \tilde{\phi}_0(\zeta)$ (i.e. independent of ζ^1). The following order terms give (3.44), but where no condition on the ζ dependence of $\tilde{g}_0$ is known. We can see using the tanh solution that $\lim_{\zeta\to\pm\infty} \partial_\zeta \tilde{\phi}_0 = 0$, and that $\lim_{\zeta\to\pm\infty}(3\tilde{\phi}_0^2 - 1) = 2$, so that

$$\frac{4}{3\sqrt{2}} \lim_{\zeta\to\pm\infty} \tilde{g}_0 = 2 \lim_{\zeta\to\pm\infty} \tilde{\phi}_1 - \lim_{\zeta\to\pm\infty} \frac{\partial^2 \tilde{\phi}_1}{\partial \zeta^2}, \tag{5.9}$$

and since $\lim_{\zeta\to\pm\infty} \tilde{\phi}_1 = \phi_1^{\pm}(0) + \zeta\, \partial_\zeta \phi_0^{\pm}(0) = \phi_1^{\pm}(0) = 0$, and $\lim_{\zeta\to\pm\infty} \tilde{g}_0 = g_0^{\pm}(0) = 0$, then we are left simply with

$$\lim_{\zeta\to\pm\infty} \frac{\partial^2 \tilde{\phi}_1}{\partial \zeta^2} = 0. \tag{5.10}$$

As before, we find a solvability condition on $\tilde{\phi}_1$ from (3.44), which in this case is

$$\int_{-\infty}^{\infty} \left[\frac{2\sqrt{2}}{3} \tilde{g}_0 - \kappa \frac{\partial \tilde{\phi}_0}{\partial \zeta} \right] \frac{\partial \tilde{\phi}_0}{\partial \zeta}\, \mathrm{d}\zeta = 0. \tag{5.11}$$

Unlike in the original conserved case, we do not know whether $\tilde{g}_0$ is a function of ζ (indeed, it is likely to be in this instance). For this non-conserved case then

$$\int_{-\infty}^{\infty} \frac{2\sqrt{2}}{3} \tilde{g}_0 \frac{\partial \tilde{\phi}_0}{\partial \zeta}\, \mathrm{d}\zeta - \kappa \int_{-\infty}^{\infty} \left[\frac{\partial \tilde{\phi}_0}{\partial \zeta} \right]^2 \mathrm{d}\zeta = \int_{-\infty}^{\infty} \frac{2\sqrt{2}}{3} \tilde{g}_0 \frac{\partial \tilde{\phi}_0}{\partial \zeta}\, \mathrm{d}\zeta - \frac{2\sqrt{2}}{3}\kappa = 0, \tag{5.12}$$

giving

$$\int_{-\infty}^{\infty} \tilde{g}_0 \frac{\partial \tilde{\phi}_0}{\partial \zeta}\, \mathrm{d}\zeta = \kappa, \tag{5.13}$$

having used the tanh solution for the leading-order phase field (3.43).

5.2.3. *Momentum equation*

The analysis of the momentum equation in inner variables follows very similarly to the original conservative case. At leading order we have $\tilde{\tau}_0^{11} = \tilde{\tau}_0^{12} = \tilde{\tau}_0^{22} = \tilde{p}_0 = 0$, $\tilde{\boldsymbol{u}}_0^+ = \tilde{\boldsymbol{u}}_0^-$, and $\partial_\zeta \tilde{\tau}_1^{12} = 0$. The following order in the momentum equation gives (3.58), where once again the difference to the CH model is that $\tilde{g}_0$ remains dependent on ζ here. Integrating (3.58) in this case, using (5.13), and matching to the outer region

https://doi.org/10.1017/jfm.2013.521 Published online by Cambridge University Press

gives the interface conditions

$$\boldsymbol{n}\cdot[\boldsymbol{\tau}_0^+ - \boldsymbol{\tau}_0^-]\cdot(\boldsymbol{I} - \boldsymbol{n}\otimes\boldsymbol{n}) = 0, \tag{5.14a}$$

$$\boldsymbol{n}\cdot[(-p_0^+ + p_0^-)\boldsymbol{I} + \boldsymbol{\tau}_0^+ - \boldsymbol{\tau}_0^-]\cdot\boldsymbol{n} = -\frac{\kappa}{Ca}. \tag{5.14b}$$

In this case the correct boundary conditions are recovered, even though the chemical potential is zero in the bulk outer regions, to all orders of Cn in the sharp-interface limit. The crucial difference is that the inner chemical potential for this non-conserved model has no restriction to its dependence on ζ, and thus it is allowed to behave as a delta function across the interface as $Cn \to 0$, whereas its behaviour must be smoother in the conserved model.

6. Body force term as $\phi\nabla g$

6.1. *Governing equations when the body force term is* $\phi\nabla g$

In the two papers of Jacqmin (1999, 2000), the diffuse-interface equations use a different form of a body force to account for the mixing of the fluids in the interface region; in our notation the body force is $-\phi\nabla g$, rather than of the form $+g\nabla\phi$ which has been used so far. The non-dimensional governing equations we consider in this section are of the form (2.12) and (2.14)–(2.15), with the momentum equation now being

$$Re\left(\frac{\partial\boldsymbol{u}}{\partial t} + \boldsymbol{u}\cdot\nabla\boldsymbol{u}\right) = -\nabla p_j + \nabla^2\boldsymbol{u} - \frac{1}{Ca}\phi\nabla g. \tag{6.1}$$

This model is formed by choosing $\alpha = 0$, $\gamma_i = 1$ and $\mathscr{C} = 0$ in the combined equation system of figure 2.

Jacqmin asserts that whilst p_j (in his notation this is written S) enforces incompressibility, it is not the pressure. We will see this clearly when considering the sharp-interface limit of this model, and then subsequently investigate the 'stress form' of the model as given by Jacqmin (1999, 2000), which does then relate the model to one with correct pressure.

6.2. *The outer region for the different body force term*

In the outer region for the bulk fluids away from the interface, we take $Cn \to 0$ using the expansions (3.1). At leading order we find

$$\nabla^2[(\phi_0^{\pm 2} - 1)\phi_0^\pm] = 0 \quad \text{and} \quad \phi_0^\pm\nabla[(\phi_0^{\pm 2} - 1)\phi_0^\pm] = \phi_0^\pm(3\phi_0^{\pm 2} - 1)\nabla\phi_0^\pm = 0, \tag{6.2}$$

which on applying $\phi_0^\pm \to \pm 1$ as the distance from the interface tends to $\pm\infty$ gives $\phi_0^\pm = \pm 1$. We then have

$$\nabla\cdot\boldsymbol{u}_0^\pm = 0, \quad Re\left(\frac{\partial\boldsymbol{u}_0^\pm}{\partial t} + \boldsymbol{u}_0^\pm\cdot\nabla\boldsymbol{u}_0^\pm\right) = -\nabla p_{j0}^\pm + \nabla^2\boldsymbol{u}_0^\pm - \frac{1}{Ca}\phi_0^\pm\nabla g_0^\pm, \tag{6.3}$$

$$\nabla^2 g_0^\pm = 0, \quad g_0^\pm = \frac{3\sqrt{2}}{4}\phi_1^\pm(3\phi_0^{\pm 2} - 1) = \frac{3\sqrt{2}}{2}\phi_1^\pm, \tag{6.4}$$

which do not immediately appear to recover the Navier–Stokes equations at leading order. For the pressure-like and body force terms to combine to form the actual pressure term expected, we need $-\nabla p_{j0}^\pm - \phi_0^\pm\nabla g_0^\pm/Ca = -\nabla p_0^\pm$, which implies $p_{j0}^\pm = p_0^\pm - \phi_0^\pm g_0^\pm/Ca$, having used $\nabla\phi_0^\pm = 0$ as $\phi_0^\pm = \pm 1$ to give $\phi_0^\pm\nabla g_0^\pm = \nabla(\phi_0^\pm g_0^\pm)$.

https://doi.org/10.1017/jfm.2013.521 Published online by Cambridge University Press

This would not be necessary if $g_0^{\pm}$ were a constant (that would have to be zero to agree with behaviour far from the interface), as $p_{j0}^{\pm}$ would then look like the pressure.

6.3. *The inner region*

The process is the same as for the CH model, and the continuity, Cahn–Hilliard type and chemical potential equations are all the same, and thus we use the results obtained earlier and consider the momentum equation where differences will arise. We note that as the Cahn–Hilliard type equation is the same as for the CH model, this model will not guarantee that no spurious diffusion can occur across the interface, although modifying the mobility to be phase field dependent as in § 4 will then give this result.

Consider the momentum equation in inner variables

$$\begin{aligned} Re\left(\frac{\partial \boldsymbol{u}}{\partial t}+(\boldsymbol{u}^s+\boldsymbol{u})\cdot\boldsymbol{\nabla}\boldsymbol{u}\right) = &-\left((1-\kappa Cn\,\zeta)^{-2}\frac{\partial p_j}{\partial \zeta^1}\boldsymbol{e}_1+\frac{1}{Cn}\frac{\partial p_j}{\partial \zeta}\boldsymbol{e}_2\right)\\ &+\begin{pmatrix} \dfrac{\partial \tau^{11}}{\partial \zeta^1}+\dfrac{1}{Cn}\dfrac{\partial \tau^{12}}{\partial \zeta}+2\Gamma^1_{11}\tau^{11}+3\Gamma^1_{12}\tau^{12} \\ \dfrac{\partial \tau^{12}}{\partial \zeta^1}+\dfrac{1}{Cn}\dfrac{\partial \tau^{22}}{\partial \zeta}+\Gamma^1_{11}\tau^{12}+\Gamma^1_{12}\tau^{22}+\Gamma^2_{11}\tau^{11} \end{pmatrix}\\ &-\frac{1}{Ca}\phi\left((1-\kappa Cn\,\zeta)^{-2}\frac{\partial g}{\partial \zeta^1}\boldsymbol{e}_1+\frac{1}{Cn}\frac{\partial g}{\partial \zeta}\boldsymbol{e}_2\right), \end{aligned} \tag{6.5}$$

where the components of $\boldsymbol{\nabla}\boldsymbol{u}$ are given in (3.26), the Christoffel symbols Γ^k_{ij} in (3.22), and the viscous stress components in (3.27), all with $\zeta^2 = Cn\,\zeta$ for the inner region. The leading order, using inner expansions (3.29), is the same as for the CH model, with differences arising at the next order, where

$$\frac{\partial \tilde{\tau}_1^{12}}{\partial \zeta}=0, \quad \frac{\partial \tilde{\tau}_1^{22}}{\partial \zeta}=\frac{\partial \tilde{p}_{j1}}{\partial \zeta}+\frac{\tilde{\phi}_0}{Ca}\frac{\partial \tilde{g}_0}{\partial \zeta}=\frac{\partial \tilde{p}_{j1}}{\partial \zeta}. \tag{6.6}$$

Integrating these equations we find

$$[\tilde{\tau}_1^{12}]_{-\infty}^{\infty}=0, \quad [\tilde{\tau}_1^{22}]_{-\infty}^{\infty}=[\tilde{p}_{j1}]_{-\infty}^{\infty}, \tag{6.7}$$

and matching to the outer region gives the interface conditions

$$\boldsymbol{n}\cdot[\boldsymbol{\tau}_0^{+}-\boldsymbol{\tau}_0^{-}]\cdot(\boldsymbol{I}-\boldsymbol{n}\otimes\boldsymbol{n})=0, \quad \boldsymbol{n}\cdot[(-p_{j0}^{+}+p_{j0}^{-})\boldsymbol{I}+\boldsymbol{\tau}_0^{+}-\boldsymbol{\tau}_0^{-}]\cdot\boldsymbol{n}=0. \tag{6.8}$$

This is the correct tangential stress balance equation, but the normal stress balance is only correct for an interface with zero curvature. For the correct normal stress balance, we may compare (6.6) to the equivalent for the original CH model (3.58). In this case we need

$$\frac{\partial \tilde{p}_{j1}}{\partial \zeta}=\frac{\partial \tilde{p}_1}{\partial \zeta}-\frac{\tilde{g}_0}{Ca}\frac{\partial \tilde{\phi}_0}{\partial \zeta}\Rightarrow 0=\frac{\partial}{\partial \zeta}\left(\tilde{p}_{j1}-\tilde{p}_1+\frac{\tilde{g}_0\tilde{\phi}_0}{Ca}\right)\Rightarrow \tilde{p}_{j1}=\tilde{p}_1-\frac{\tilde{g}_0\tilde{\phi}_0}{Ca}, \tag{6.9}$$

using the fact that $\tilde{g}_0$ is independent of ζ. This then agrees with the suggestion from the outer region, and gives the interface conditions

$$\boldsymbol{n}\cdot[\boldsymbol{\tau}_0^{+}-\boldsymbol{\tau}_0^{-}]\cdot(\boldsymbol{I}-\boldsymbol{n}\otimes\boldsymbol{n})=0, \quad \boldsymbol{n}\cdot[(-p_0^{+}+p_0^{-})\boldsymbol{I}+\boldsymbol{\tau}_0^{+}-\boldsymbol{\tau}_0^{-}]\cdot\boldsymbol{n}=-\frac{\kappa}{Ca}, \tag{6.10}$$

as expected. It is of interest that this relationship between pressures is not quite the same as that suggested by Jacqmin (1999), which contains other terms involving ϕ

https://doi.org/10.1017/jfm.2013.521 Published online by Cambridge University Press

and $|\nabla\phi|^2$. Next we will consider the various suggestions of Jacqmin (1999, 2000) about the form of the stress tensor and pressure.

7. Other constant mobility models

Following on from the previous section, we consider the model as suggested by Jacqmin (1999), where the model is as in the previous section, but with

$$p_j = p - \frac{g\phi}{Ca} + \frac{3\sqrt{2}}{16Ca}\left[\frac{(\phi^2-1)^2}{Cn} - 2Cn|\nabla\phi|^2\right]. \tag{7.1}$$

This affects the momentum equation, which now becomes

$$Re\left(\frac{\partial \boldsymbol{u}}{\partial t} + \boldsymbol{u}\cdot\nabla\boldsymbol{u}\right) = -\nabla p + \nabla^2\boldsymbol{u} + \frac{g\nabla\phi}{Ca} - \frac{3\sqrt{2}}{16Ca}\nabla\left[\frac{(\phi^2-1)^2}{Cn} - 2Cn|\nabla\phi|^2\right], \tag{7.2}$$

and we can also verify that the 'stress form' of the model (Jacqmin 1999, 2000) is in agreement. This stress form has the momentum equation

$$Re\left(\frac{\partial \boldsymbol{u}}{\partial t} + \boldsymbol{u}\cdot\nabla\boldsymbol{u}\right) = -\nabla p + \nabla^2\boldsymbol{u} + \nabla\cdot\boldsymbol{\tau}_j, \quad \boldsymbol{\tau}_j = \frac{3\sqrt{2}}{4}\frac{Cn}{Ca}\begin{bmatrix}\left(\dfrac{\partial\phi}{\partial y}\right)^2 & -\dfrac{\partial\phi}{\partial x}\dfrac{\partial\phi}{\partial y}\\ -\dfrac{\partial\phi}{\partial x}\dfrac{\partial\phi}{\partial y} & \left(\dfrac{\partial\phi}{\partial x}\right)^2\end{bmatrix}, \tag{7.3}$$

and this is equivalent to (7.2) as

$$\begin{aligned}&\frac{g\nabla\phi}{Ca} - \frac{3\sqrt{2}}{16Ca}\nabla\left[\frac{(\phi^2-1)^2}{Cn} - 2Cn|\nabla\phi|^2\right]\\ &\quad= \frac{3\sqrt{2}}{4}\frac{Cn}{Ca}\begin{pmatrix}\dfrac{\partial\phi}{\partial y}\dfrac{\partial^2\phi}{\partial x\partial y} - \dfrac{\partial\phi}{\partial x}\dfrac{\partial^2\phi}{\partial y^2}\\ \dfrac{\partial\phi}{\partial x}\dfrac{\partial^2\phi}{\partial x\partial y} - \dfrac{\partial\phi}{\partial y}\dfrac{\partial^2\phi}{\partial x^2}\end{pmatrix} = \nabla\cdot\boldsymbol{\tau}_j.\end{aligned} \tag{7.4}$$

Observing the apparently non-trivial difference between this model and the original CH model, as used by Qian *et al.* (2006) and Yue *et al.* (2010), we consider other forms of binary fluid models in the literature to see if a general form can be observed. There are two other forms of note: the model used by Khatavkar *et al.* (2006, 2007) and the binary fluid model described in the prominent review paper by Anderson *et al.* (1998).

The model of Khatavkar *et al.* (2006, 2007) in our setting and with our notation has the same continuity, Cahn–Hilliard type and chemical potential equations, but with the momentum equation now being

$$Re\left(\frac{\partial \boldsymbol{u}}{\partial t} + \boldsymbol{u}\cdot\nabla\boldsymbol{u}\right) = -\nabla p + \nabla^2\boldsymbol{u} + \frac{g\nabla\phi}{Ca} - \frac{3\sqrt{2}}{16Ca}\nabla\left[\frac{(\phi^2-1)^2}{Cn} + 2Cn|\nabla\phi|^2\right], \tag{7.5}$$

the crucial difference to the Jacqmin model above being the sign of the $2Cn|\nabla\phi|^2$ term. Of interest are the additional terms from the Navier–Stokes equations, as these

https://doi.org/10.1017/jfm.2013.521 Published online by Cambridge University Press

may be written in the more compact form

$$\frac{g\nabla\phi}{Ca} - \frac{3\sqrt{2}}{16Ca}\nabla\left[\frac{(\phi^2-1)^2}{Cn} + 2Cn|\nabla\phi|^2\right] = -\frac{3\sqrt{2}}{4}\frac{Cn}{Ca}\left[(\nabla^2\phi)\nabla\phi + \frac{1}{2}\nabla\left(|\nabla\phi|^2\right)\right]$$
$$= -\frac{3\sqrt{2}}{4}\frac{Cn}{Ca}\nabla\cdot(\nabla\phi\otimes\nabla\phi)\,. \tag{7.6}$$

Note that this last description matches the additional term in the momentum equation of the non-conservative formulation of Yang *et al.* (2006), being part of the stress in (5) there (it has already been noted in § 5 that both cited non-conservative models had slightly different formulations to the one investigated). In § 5, we used a formulation to consider a non-conservative Allen–Cahn type behaviour where comparisons to the CH model could be drawn. The model of Yang *et al.* (2006) also includes a numerically evaluated Lagrange multiplier to enforce volume fraction conservation, the effect of which is beyond the scope of the present work.

The other similar binary-fluid model, given in the review paper by Anderson *et al.* (1998), in our setting and with our notation has the non-dimensional momentum equation

$$Re\left(\frac{\partial\boldsymbol{u}}{\partial t} + \boldsymbol{u}\cdot\nabla\boldsymbol{u}\right) = -\nabla p + \nabla^2\boldsymbol{u} + \frac{3\sqrt{2}}{4}\frac{Cn}{Ca}\nabla\cdot\left[\frac{1}{2}|\nabla\phi|^2\boldsymbol{I} - \nabla\phi\otimes\nabla\phi\right]. \tag{7.7}$$

Once again, it is of most interest to consider the terms additional to the Navier–Stokes equations, those being

$$\frac{3\sqrt{2}}{4}\frac{Cn}{Ca}\nabla\cdot\left[\frac{1}{2}|\nabla\phi|^2\boldsymbol{I} - \nabla\phi\otimes\nabla\phi\right] = \frac{g\nabla\phi}{Ca} - \frac{3\sqrt{2}}{16Ca}\nabla\left[\frac{(\phi^2-1)^2}{Cn}\right], \tag{7.8}$$

at which point it is clear that these models can be put into a general form, being (2.12), (2.14)–(2.15) with

$$Re\left(\frac{\partial\boldsymbol{u}}{\partial t} + \boldsymbol{u}\cdot\nabla\boldsymbol{u}\right) = -\nabla p + \nabla^2\boldsymbol{u} + \frac{g\nabla\phi}{Ca} - \frac{3\mathscr{B}\sqrt{2}}{16Ca}\nabla\left[\frac{(\phi^2-1)^2}{Cn} + \mathscr{G}Cn|\nabla\phi|^2\right], \tag{7.9}$$

where $\mathscr{G}=-2$, $\mathscr{B}=1$ corresponds to the Jacqmin (1999, 2000) models, as well as similar forms in early works such as by Starovoitov (1994) and Antanovskii (1995). When $\mathscr{G}=2$, $\mathscr{B}=1$, this corresponds to the model of Khatavkar *et al.* (2006, 2007), and when $\mathscr{G}=0$, $\mathscr{B}=1$, then the Anderson *et al.* (1998) model is obtained. Finally, when $\mathscr{B}=0$, the CH model used by many authors and already analysed, is recovered. Note that the Anderson *et al.* version can be viewed as a modification of the 'body force' in the CH model, $\boldsymbol{b}_m$, that is,

$$\boldsymbol{b}_m = \left[g - \frac{3\sqrt{2}}{4Cn}(\phi^2-1)\phi\right]\frac{\nabla\phi}{Ca}. \tag{7.10}$$

Note also that this general model corresponds to $\gamma_i=1$, $\alpha=0$, and $\mathscr{C}=1$ in figure 2.

7.1. *Outer region of general model*

In the outer region for the bulk fluids away from the interface with expansions (3.1), the leading orders as $Cn\to 0$, $O(Cn^{-1})$ and $O(1)$, recover the same classical

https://doi.org/10.1017/jfm.2013.521 Published online by Cambridge University Press

Navier–Stokes equations and Laplace equation for the leading-order chemical potential for any $\mathscr{G}$ and $\mathscr{B}$, having eliminated a term of the form $-3\sqrt{2}\mathscr{B}\phi_0^{\pm}(\phi_0^{\pm 2}-1)\nabla\phi_1^{\pm}/(4Ca)$ as $\phi_0^{\pm}=\pm 1$. The next order, $O(Cn)$, gives

$$\nabla\cdot\boldsymbol{u}_1^{\pm}=0, \quad \frac{4}{3\sqrt{2}}g_0^{\pm}=\phi_1^{\pm}(3\phi_0^{\pm 2}-1)=2\phi_1^{\pm}, \quad \frac{\partial\phi_1^{\pm}}{\partial t}+\boldsymbol{u}_0^{\pm}\cdot\nabla\phi_1^{\pm}=\beta\nabla^2 g_1^{\pm}, \tag{7.11}$$

$$Re\left(\frac{\partial\boldsymbol{u}_1^{\pm}}{\partial t}+\boldsymbol{u}_0^{\pm}\cdot\nabla\boldsymbol{u}_1^{\pm}+\boldsymbol{u}_1^{\pm}\cdot\nabla\boldsymbol{u}_0^{\pm}\right)=-\nabla p_1^{\pm}+\nabla^2\boldsymbol{u}_1^{\pm}+\frac{\nabla\phi_1^{\pm}}{Ca}\left[g_0^{\pm}-\frac{3\mathscr{B}\sqrt{2}}{2}\phi_1^{\pm}\right], \tag{7.12}$$

and crucially for the models where $\mathscr{B}=1$, combining the result for $g_0^{\pm}$ with the momentum equation leaves a linearized version of the Navier–Stokes equations without additional terms to this order (without requiring any condition on either $\mathscr{G}$ or $g_0^{\pm}$). When $\mathscr{B}=0$, as for the CH model, then $g_0^{\pm}=0$ is required for only classical terms to be at this order, as seen earlier, and causes the restriction on the model as discussed in § 3.2.

For interest, we continue to $O(Cn^2)$, and find that the non-classical terms in the momentum equation are

$$\frac{1}{Ca}\left[\left(g_0^{\pm}-\frac{3\mathscr{B}\sqrt{2}}{2}\phi_1^{\pm}\right)\nabla\phi_2^{\pm}+\left(g_1^{\pm}-\frac{3\mathscr{B}\sqrt{2}}{4}\left\{3\phi_0^{\pm}\phi_1^{\pm 2}+2\phi_2^{\pm}\right\}\right)\nabla\phi_1^{\pm}\right], \tag{7.13}$$

where $g_1^{\pm}=3\sqrt{2}(3\phi_0^{\pm}\phi_1^{\pm 2}+2\phi_2^{\pm})/4$, and hence once again these additional non-classical terms cancel when $\mathscr{B}=1$, and only terms involved in the linearized Navier–Stokes equations remain. At $O(Cn^3)$ this feature breaks down, as terms of forms $\nabla^2\phi_1^{\pm}\nabla\phi_1^{\pm}$ and $\nabla(|\nabla\phi_1^{\pm}|^2)$ enter and do not cancel, regardless of the choice of $\mathscr{G}$ or $\mathscr{B}$. At this order the chemical potential equation yields $g_2^{\pm}=3\sqrt{2}[\left(6\phi_0^{\pm}\phi_1^{\pm}\phi_2^{\pm}+\phi_1^{\pm 3}+2\phi_3^{\pm}\right)-\nabla^2\phi_1^{\pm}]/4$, and the non-classical terms in the momentum equation are

$$\begin{aligned}\frac{3\sqrt{2}}{4Ca}[\{1-\mathscr{B}\}\{2\phi_1^{\pm}\nabla\phi_3^{\pm}+(2\phi_2^{\pm}+3\phi_0^{\pm}\phi_1^{\pm 2})\nabla\phi_2^{\pm}\\ +(6\phi_0^{\pm}\phi_1^{\pm}\phi_2^{\pm}+\phi_1^{\pm 3}+2\phi_3^{\pm})\nabla\phi_1^{\pm}\}-\nabla^2\phi_1^{\pm}\nabla\phi_1^{\pm}-\mathscr{G}\mathscr{B}\nabla(|\nabla\phi_1^{\pm}|^2)].\end{aligned} \tag{7.14}$$

7.2. *Inner region of general model*

In the inner region, the only equation that has changed from the CH model is the momentum equation. Once again, this means that to guarantee that no spurious diffusion can occur, a phase field dependent mobility as in § 4 should be used. However, we continue with a constant mobility here, as in the CH model, and as used by the various authors cited earlier in this section. The additional term in the momentum equation, compared to the CH analysis, is

$$-\frac{3\mathscr{B}\sqrt{2}}{16Ca}\nabla\left[\frac{(\phi^2-1)^2}{Cn}+\mathscr{G}Cn|\nabla\phi|^2\right]=-\frac{3\mathscr{B}\sqrt{2}}{16Ca}\begin{pmatrix}\mathfrak{A}^1\\ \mathfrak{A}^2\end{pmatrix}, \tag{7.15}$$

where

$$\mathfrak{A}^1=\frac{1}{(1-\kappa Cn\,\zeta)^2}\frac{\partial}{\partial\zeta^1}\left(\frac{(\phi^2-1)^2}{Cn}+\mathscr{G}Cn\left[(1-\kappa Cn\,\zeta)^{-2}\left(\frac{\partial\phi}{\partial\zeta^1}\right)^2+\frac{1}{Cn^2}\left(\frac{\partial\phi}{\partial\zeta}\right)^2\right]\right), \tag{7.16a}$$

https://doi.org/10.1017/jfm.2013.521 Published online by Cambridge University Press

$$\mathfrak{A}^2 = \frac{1}{Cn}\frac{\partial}{\partial\zeta}\left(\frac{(\phi^2-1)^2}{Cn} + \mathscr{G}Cn\left[(1-\kappa Cn\,\zeta)^{-2}\left(\frac{\partial\phi}{\partial\zeta^1}\right)^2 + \frac{1}{Cn^2}\left(\frac{\partial\phi}{\partial\zeta}\right)^2\right]\right), \tag{7.16b}$$

and thus the additional terms at $O(Cn^{-2})$ are

$$\begin{aligned}
&-\frac{3\mathscr{B}\sqrt{2}}{16Ca}\begin{pmatrix}0\\ \dfrac{\partial}{\partial\zeta}\left[(\tilde{\phi}_0^2-1)^2 + \mathscr{G}\left(\dfrac{\partial\tilde{\phi}_0}{\partial\zeta}\right)^2\right]\end{pmatrix}\\
&\quad= -\frac{3\mathscr{B}\sqrt{2}}{8Ca}\begin{pmatrix}0\\ \dfrac{\partial\tilde{\phi}_0}{\partial\zeta}\left(\mathscr{G}\dfrac{\partial^2\tilde{\phi}_0}{\partial\zeta^2} + 2\tilde{\phi}_0(\tilde{\phi}_0^2-1)\right)\end{pmatrix}\\
&\quad= -\frac{3\mathscr{B}\sqrt{2}}{8Ca}\begin{pmatrix}0\\ (\mathscr{G}+2)\dfrac{\partial\tilde{\phi}_0}{\partial\zeta}\dfrac{\partial^2\tilde{\phi}_0}{\partial\zeta^2}\end{pmatrix},
\end{aligned} \tag{7.17}$$

having used (3.42). At leading order the first equation in the momentum is once again $\partial_\zeta\tilde{\tau}_0^{12} = 0$, where $\tilde{\tau}_0^{12} = \partial_\zeta\tilde{u}_0^1$, which thus gives $\tilde{\boldsymbol{u}}_0^+ = \tilde{\boldsymbol{u}}_0^-$ as in previous cases when coupled to the results from the other equations, but the second momentum equation now has an additional term, that is,

$$\begin{aligned}
0 &= \frac{\partial}{\partial\zeta}(-\tilde{p}_0 + \tilde{\tau}_0^{22}) - \frac{3\mathscr{B}\sqrt{2}}{8Ca}(2+\mathscr{G})\frac{\partial\tilde{\phi}_0}{\partial\zeta}\frac{\partial^2\tilde{\phi}_0}{\partial\zeta^2}\\
&= \frac{\partial}{\partial\zeta}\left(-\tilde{p}_0 + \tilde{\tau}_0^{22} - \frac{3\mathscr{B}\sqrt{2}}{32Ca}(2+\mathscr{G})(\tilde{\phi}_0^2-1)^2\right),
\end{aligned} \tag{7.18}$$

where $\tilde{\tau}_0^{22} = 2\partial_\zeta\tilde{u}_0^2 = 0$, as $\tilde{u}_0^2$ is independent of ζ, and using (B 3) in the simplification. On integrating and setting the arbitrary function equal to zero (by considering the matching behaviour as $\zeta\to\pm\infty$, where $\lim_{\zeta\to\pm\infty}\tilde{\boldsymbol{\tau}}_0 = 0$, $\lim_{\zeta\to\pm\infty}\tilde{p}_0 = 0$, and $\lim_{\zeta\to\pm\infty}\tilde{\phi}_0 = \pm1$), we have

$$\tilde{p}_0 = -\frac{3\mathscr{B}\sqrt{2}}{32Ca}(2+\mathscr{G})(\tilde{\phi}_0^2-1)^2. \tag{7.19}$$

The next order, $O(Cn^{-1})$, in the momentum equation then suggests

$$\begin{aligned}
\mathbf{0} = &-\begin{pmatrix}\dfrac{\partial\tilde{p}_0}{\partial\zeta^1}\\ \dfrac{\partial\tilde{p}_1}{\partial\zeta}\end{pmatrix} + \begin{pmatrix}\dfrac{\partial\tilde{\tau}_1^{12}}{\partial\zeta}\\ \dfrac{\partial\tilde{\tau}_1^{22}}{\partial\zeta}\end{pmatrix} + \frac{\tilde{g}_0}{Ca}\frac{\partial\tilde{\phi}_0}{\partial\zeta}\boldsymbol{e}_2\\
&-\frac{3\mathscr{B}\sqrt{2}}{4Ca}\left(\left[(3\tilde{\phi}_0^2-1)\tilde{\phi}_1 + \frac{\mathscr{G}}{2}\frac{\partial^2\tilde{\phi}_1}{\partial\zeta^2}\right]\frac{\partial\tilde{\phi}_0}{\partial\zeta} + \frac{\mathscr{G}+2}{2}\frac{\partial^2\tilde{\phi}_0}{\partial\zeta^2}\frac{\partial\tilde{\phi}_1}{\partial\zeta}\right)\boldsymbol{e}_2,
\end{aligned} \tag{7.20}$$

https://doi.org/10.1017/jfm.2013.521 Published online by Cambridge University Press

where the final term contains the differences from the CH model, which at this order are

$$-\frac{3\mathscr{B}\sqrt{2}}{16Ca}\begin{pmatrix}\dfrac{\partial}{\partial\zeta^1}\left[(\tilde{\phi}_0^2-1)^2+\mathscr{G}\left(\dfrac{\partial\tilde{\phi}_0}{\partial\zeta}\right)^2\right]\\ \dfrac{\partial}{\partial\zeta}\left[4(\tilde{\phi}_0^2-1)\tilde{\phi}_0\tilde{\phi}_1+2\mathscr{G}\dfrac{\partial\tilde{\phi}_0}{\partial\zeta}\dfrac{\partial\tilde{\phi}_1}{\partial\zeta}\right]\end{pmatrix}$$
$$=-\frac{3\mathscr{B}\sqrt{2}}{4Ca}\begin{pmatrix}0\\ \dfrac{\partial}{\partial\zeta}\left[(\tilde{\phi}_0^2-1)\tilde{\phi}_0\tilde{\phi}_1+\dfrac{\mathscr{G}}{2}\dfrac{\partial\tilde{\phi}_0}{\partial\zeta}\dfrac{\partial\tilde{\phi}_1}{\partial\zeta}\right]\end{pmatrix}, \tag{7.21}$$

and the previous result follows. We may now combine this with the known results from the original model to see how these extra terms affect our analysis. We have the first equation giving

$$\frac{\partial\tilde{p}_0}{\partial\zeta^1}=\frac{\partial\tilde{\tau}_1^{12}}{\partial\zeta}, \tag{7.22}$$

which on using the form for $\tilde{p}_0$ above, in (7.19) – which clearly shows $\tilde{p}_0=\tilde{p}_0(\zeta)$, since $\tilde{\phi}_0=\tilde{\phi}_0(\zeta)$ – then

$$\frac{\partial\tilde{\tau}_1^{12}}{\partial\zeta}=0, \tag{7.23}$$

and the classical tangential stress balance follows as for the CH model. For the second equation we have

$$-\frac{\partial\tilde{p}_1}{\partial\zeta}+\frac{\partial\tilde{\tau}_1^{22}}{\partial\zeta}+\frac{\tilde{g}_0}{Ca}\frac{\partial\tilde{\phi}_0}{\partial\zeta}-\frac{3\mathscr{B}\sqrt{2}}{4Ca}\frac{\partial}{\partial\zeta}\left[(\tilde{\phi}_0^2-1)\tilde{\phi}_0\tilde{\phi}_1+\frac{\mathscr{G}}{2}\frac{\partial\tilde{\phi}_0}{\partial\zeta}\frac{\partial\tilde{\phi}_1}{\partial\zeta}\right]=0, \tag{7.24}$$

and integrating this from $\zeta=-\infty\cdots\infty$ gives

$$-[\tilde{p}_1]_{-\infty}^{\infty}+[\tilde{\tau}_1^{22}]_{-\infty}^{\infty}+\int_{-\infty}^{\infty}\frac{\tilde{g}_0}{Ca}\frac{\partial\tilde{\phi}_0}{\partial\zeta}\,\mathrm{d}\zeta$$
$$-\frac{3\mathscr{B}\sqrt{2}}{4Ca}\left[(\tilde{\phi}_0^2-1)\tilde{\phi}_0\tilde{\phi}_1+\frac{\mathscr{G}}{2}\frac{\partial\tilde{\phi}_0}{\partial\zeta}\frac{\partial\tilde{\phi}_1}{\partial\zeta}\right]_{-\infty}^{\infty}=0. \tag{7.25}$$

Using the equation for $\tilde{g}_0$ (as in (3.44)), following the same process as for the CH model, and noticing that the final term is zero as $\lim_{\zeta\to\pm\infty}\tilde{\phi}_0^2=1$ and $\lim_{\zeta\to\pm\infty}\partial_\zeta\tilde{\phi}_0=0$, this then simplifies to

$$-[\tilde{p}_1]_{-\infty}^{\infty}+[\tilde{\tau}_1^{22}]_{-\infty}^{\infty}+\frac{\kappa}{Ca}=0, \tag{7.26}$$

and finally matching this to the outer regions leads to

$$\boldsymbol{n}\cdot[(-p_0^++p_0^-)\boldsymbol{I}+\boldsymbol{\tau}_0^+-\boldsymbol{\tau}_0^-]\cdot\boldsymbol{n}=-\frac{\kappa}{Ca}. \tag{7.27}$$

These results show that all of the classical conditions are recovered for this model in the sharp-interface limit, and the pressure in the full model can be asymptotically

https://doi.org/10.1017/jfm.2013.521 Published online by Cambridge University Press

connected to the continuum pressure regardless of the choice of $\mathscr{G}$. In the bulk regions we must have $\mathscr{B} = 1$ for the classical equations to hold up to and including $O(Cn^2)$.

Considering the specific cases of $\mathscr{G} = \{-2, 0, 2\}$ with $\mathscr{B} = 1$ for the Jacqmin, Anderson *et al.*, and Khatavkar *et al.* models respectively, there is no reason to pick any in particular for convergence in the sharp-interface limit (or indeed to pick any of these three). However, we note the interesting differences in the final calculation for the inner region momentum at $O(Cn^{-1})$. From (7.20) the second equation is

$$-\frac{\partial \tilde{p}_1}{\partial \zeta} + \frac{\partial \tilde{\tau}_1^{22}}{\partial \zeta} + \frac{\tilde{g}_0}{Ca}\frac{\partial \tilde{\phi}_0}{\partial \zeta} - \frac{3\mathscr{B}\sqrt{2}}{4Ca}\left(\left[(3\tilde{\phi}_0^2 - 1)\tilde{\phi}_1 + \frac{\mathscr{G}}{2}\frac{\partial^2 \tilde{\phi}_1}{\partial \zeta^2}\right]\frac{\partial \tilde{\phi}_0}{\partial \zeta} + \frac{\mathscr{G}+2}{2}\frac{\partial^2 \tilde{\phi}_0}{\partial \zeta^2}\frac{\partial \tilde{\phi}_1}{\partial \zeta}\right) = 0, \quad (7.28)$$

and using $\tilde{g}_0$ from (3.44), this is

$$-\frac{\partial \tilde{p}_1}{\partial \zeta} + \frac{\partial \tilde{\tau}_1^{22}}{\partial \zeta} + \frac{3\sqrt{2}}{4Ca}\left\{\left[(3\tilde{\phi}_0^2 - 1)\tilde{\phi}_1(1-\mathscr{B}) - \left(1 + \frac{\mathscr{G}\mathscr{B}}{2}\right)\frac{\partial^2 \tilde{\phi}_1}{\partial \zeta^2}\right]\frac{\partial \tilde{\phi}_0}{\partial \zeta} + \kappa\left(\frac{\partial \tilde{\phi}_0}{\partial \zeta}\right)^2 - \mathscr{B}\left(\frac{\mathscr{G}+2}{2}\right)\frac{\partial^2 \tilde{\phi}_0}{\partial \zeta^2}\frac{\partial \tilde{\phi}_1}{\partial \zeta}\right\} = 0. \quad (7.29)$$

For $\mathscr{B} = 1$ this is therefore

$$-\frac{\partial \tilde{p}_1}{\partial \zeta} + \frac{\partial \tilde{\tau}_1^{22}}{\partial \zeta} + \frac{3\sqrt{2}}{4Ca}\left\{\kappa\left(\frac{\partial \tilde{\phi}_0}{\partial \zeta}\right)^2 - \frac{2+\mathscr{G}}{2}\frac{\partial}{\partial \zeta}\left(\frac{\partial \tilde{\phi}_1}{\partial \zeta}\frac{\partial \tilde{\phi}_0}{\partial \zeta}\right)\right\} = 0, \quad (7.30)$$

and integrating gives

$$[\tilde{p}_1]_{-\infty}^{\infty} - [\tilde{\tau}_1^{22}]_{-\infty}^{\infty} = \frac{\kappa}{Ca} - \frac{3\sqrt{2}}{4Ca}\frac{2+\mathscr{G}}{2}\left[\frac{\partial \tilde{\phi}_1}{\partial \zeta}\frac{\partial \tilde{\phi}_0}{\partial \zeta}\right]_{-\infty}^{\infty}. \quad (7.31)$$

As before, we see that any value of $\mathscr{G}$ will lead to the correct normal stress boundary condition, but $\mathscr{G} = -2$ is special in that it does not require the argument that $\lim_{\zeta \to \pm\infty} \partial_\zeta \tilde{\phi}_0 = 0$, although that is used elsewhere in the inner region.

For numerical implementation, the choice of $\mathscr{G}$ should have no effect on the ability to approach a sharp-interface limit, and thus would not be expected to give any benefit as a fitting parameter. It may, however, be determined for ease or speed of calculation. In the case $\mathscr{G} = 0$ the non-classical terms are most simply written in the 'body force' form of (7.10), although g must still be calculated separately, whereas $\mathscr{G} = 2$ reduces to the compact final form in (7.6). For $\mathscr{G} = -2$ the forms of (7.4) look less compact, but may have advantages in terms of computational ease depending on the efficiency of certain operations and the numerical methods implemented.

8. Tensorial mobility

8.1. *Governing equations with tensorial mobility*

We consider the governing equations when the mobility has a tensorial form, specifically $\gamma = \gamma_T(\boldsymbol{I} - \hat{\boldsymbol{n}} \otimes \hat{\boldsymbol{n}})$, motivated by Gugenberger *et al.* (2008), and we note that a similar tensorial construction is considered by Nicoli, Plapp & Henry (2011), both

https://doi.org/10.1017/jfm.2013.521 Published online by Cambridge University Press

used in phase field models for problems without coupling to hydrodynamic equations. This suggests that diffusion occurs in the tangential direction to the interface, which could be considered to be physically motivated for immiscible fluids, where diffusion in all directions near to the interface could not be expected to be perfectly uniform. Here the quantity $\hat{\boldsymbol{n}}$ is the unit normal on any curve defined by constant ϕ, hence

$$\hat{\boldsymbol{n}} = -\frac{\breve{\nabla}\phi}{|\breve{\nabla}\phi|} \quad \text{and thus} \quad \hat{\boldsymbol{n}} \otimes \hat{\boldsymbol{n}} = \frac{\breve{\nabla}\phi \otimes \breve{\nabla}\phi}{|\breve{\nabla}\phi|^2}. \tag{8.1}$$

In non-dimensional form, the governing equations are (2.12)–(2.14), with

$$\frac{\partial \phi}{\partial t} + \boldsymbol{u} \cdot \nabla \phi = \beta \nabla \cdot ((\boldsymbol{I} - \hat{\boldsymbol{n}} \otimes \hat{\boldsymbol{n}}) \nabla g), \tag{8.2}$$

where $\beta = \gamma_T \sigma / L^2 U$ has been slightly redefined, and the other non-dimensional parameters remain as in previous cases.

In the outer region we take the usual expansions (3.1), and at leading order in the Cahn–Hilliard type equation when substituting the chemical potential form, we have at $O(Cn^{-1})$

$$\nabla \cdot \left\{ \left(\boldsymbol{I} - \frac{\nabla \phi_0^{\pm} \otimes \nabla \phi_0^{\pm}}{|\nabla \phi_0^{\pm}|^2} \right) \nabla \left[(\phi_0^{\pm 2} - 1) \phi_0^{\pm} \right] \right\} = 0, \tag{8.3}$$

and the left-hand side may be seen to be automatically zero after some algebra. As this is zero, we cannot determine the leading-order values for the order parameter, a problem encountered in the model without hydrodynamics by Gugenberger *et al.* (2008) and requiring modification of the tensorial form. Unlike there, however, we have other equations to consider, and the momentum equations at $O(Cn^{-1})$ are

$$\frac{1}{Ca} \frac{3\sqrt{2}}{4} (\phi_0^{\pm 2} - 1) \phi_0^{\pm} \nabla \phi_0^{\pm} = 0, \tag{8.4}$$

which, along with the requirement that $\phi_0^{\pm} \to \pm 1$ as the distance from the interface increases to $\pm\infty$, determines $\phi_0^{\pm} = \pm 1$. At $O(1)$, we find the linearized Navier–Stokes equations (3.2)–(3.3), and for the Cahn–Hilliard type equation we have $0 = O(Cn)$ (details of this calculation are in appendix C). The next order gives

$$\nabla \cdot \boldsymbol{u}_1^{\pm} = 0, \tag{8.5}$$

$$Re \left(\frac{\partial \boldsymbol{u}_1^{\pm}}{\partial t} + \boldsymbol{u}_0^{\pm} \cdot \nabla \boldsymbol{u}_1^{\pm} + \boldsymbol{u}_1^{\pm} \cdot \nabla \boldsymbol{u}_0^{\pm} \right) = -\nabla p_1^{\pm} + \nabla^2 \boldsymbol{u}_1^{\pm} + \frac{3\sqrt{2}}{2Ca} \phi_1^{\pm} \nabla \phi_1^{\pm}, \tag{8.6}$$

$$\frac{\partial \phi_1^{\pm}}{\partial t} + \boldsymbol{u}_0^{\pm} \cdot \nabla \phi_1^{\pm} = \beta \frac{3\sqrt{2}}{2} \nabla \cdot \left[\left(\boldsymbol{I} - \frac{\nabla \phi_1^{\pm} \otimes \nabla \phi_1^{\pm}}{|\nabla \phi_1^{\pm}|^2} \right) \nabla \phi_2^{\pm} \right], \tag{8.7}$$

where it may be clearly seen that $\phi_1^{\pm}$ must be a constant, or zero (indeed, as we would require $\phi_1^{\pm} \to 0$ as the distance to the interface increases, it would have to be zero), for any non-classical effects to be negligible at this order. Unlike for the scalar phase field case, the inner region will not prescribe a connection between $g_0^{\pm}$ (or $\phi_1^{\pm}$) and the curvature of the interface κ, and thus these terms may be zero for curved interfaces. Indeed, an outer solution of $g = g^{\pm} = 0$ and $\phi = \phi^{\pm} = \pm 1$ is consistent with the classical interface conditions to all orders in Cn.

https://doi.org/10.1017/jfm.2013.521 Published online by Cambridge University Press

8.2. *The inner region*

As for the CH model, the leading-order continuity equation gives that $\tilde{u}_0^2$ is independent of ζ. The significant differences will occur in the Cahn–Hilliard type equation, which in body-fitted coordinates in the inner region is

$$\frac{\partial \phi}{\partial t} + (\boldsymbol{u}^s + \boldsymbol{u}) \cdot \left[(1 - \kappa Cn\, \zeta)^{-2} \frac{\partial \phi}{\partial \zeta^1} \boldsymbol{e}_1 + \frac{1}{Cn} \frac{\partial \phi}{\partial \zeta} \boldsymbol{e}_2 \right] = \beta \left\{ \frac{1}{Cn} \frac{\partial \lambda_2}{\partial \zeta} - \frac{\kappa \lambda_2}{1 - \kappa Cn\, \zeta} + \frac{\partial \lambda_1}{\partial \zeta^1} - \frac{Cn \lambda_1 \zeta}{1 - \kappa Cn\, \zeta} \frac{\partial \kappa}{\partial \zeta^1} \right\}, \tag{8.8}$$

where

$$\boldsymbol{\lambda} = \begin{pmatrix} \lambda_1 \\ \lambda_2 \end{pmatrix} = \left(\boldsymbol{I} - \frac{\nabla \phi \otimes \nabla \phi}{|\nabla \phi|^2} \right) \nabla g = \begin{pmatrix} \dfrac{\partial \tilde{g}_0}{\partial \zeta^1} - \left(\dfrac{\partial \tilde{\phi}_0}{\partial \zeta} \right)^{-1} \dfrac{\partial \tilde{\phi}_0}{\partial \zeta^1} \dfrac{\partial \tilde{g}_0}{\partial \zeta} \\ 0 \end{pmatrix} + O(Cn), \tag{8.9}$$

having used expansions (3.29); for further details see appendix C. This means that there is no $O(Cn^{-2})$ term in the expansion of this Cahn–Hilliard type equation, and thus no restriction on $\tilde{g}_0$ being independent of ζ is imposed. This then resolves the issue with the original model, where $\tilde{g}_0 = \kappa = 0$ if $g_0^{\pm} = 0$ is imposed in the outer region.

The leading-order equation is thus at $O(Cn^{-1})$, and is

$$\frac{\partial \tilde{\phi}_0}{\partial \zeta} (\boldsymbol{u}^s + \tilde{\boldsymbol{u}}_0) \cdot \boldsymbol{e}_2 = \beta \frac{\partial}{\partial \zeta} (0), \tag{8.10}$$

which gives that $u_n^s = -u_0^{2\pm}$, with no possibility of any spurious diffusion at this order, without any further modification of the mobility from the tensorial form considered here (that is, in particular, with no need to have an additional multiplicative term like those in § 4). This then leads to the expected kinematic boundary condition for the sharp interface defined by $\zeta^2 = 0$.

It remains to analyse the chemical potential and momentum equations for this model. The chemical potential equation is as for the CH model, in particular giving (3.43)–(3.44) for the leading-order phase field and chemical potential, respectively. The momentum equations also follow as for the original case initially, but we have the crucial difference that here nothing is known about the dependence of ζ on $\tilde{g}_0$.

At leading order the same results hold as for the CH model, where $\tilde{\tau}_0^{11} = \tilde{\tau}_0^{12} = \tilde{\tau}_0^{22} = \tilde{p}_0 = 0$, and $\tilde{\boldsymbol{u}}_0^+ = \tilde{\boldsymbol{u}}_0^-$. Similarly, the next order in the momentum equation then suggests

$$\frac{\partial \tilde{\tau}_1^{12}}{\partial \zeta} = 0, \quad \frac{\partial \tilde{\tau}_1^{22}}{\partial \zeta} = \frac{\partial \tilde{p}_1}{\partial \zeta} - \frac{\tilde{g}_0}{Ca} \frac{\partial \tilde{\phi}_0}{\partial \zeta}. \tag{8.11}$$

Integrating the equations for the next-order momentum equations, we find

$$[\tilde{\tau}_1^{12}]_{-\infty}^{\infty} = 0, \quad [\tilde{\tau}_1^{22}]_{-\infty}^{\infty} = [\tilde{p}_1]_{-\infty}^{\infty} - \frac{1}{Ca} \int_{-\infty}^{\infty} \tilde{g}_0 \frac{\partial \tilde{\phi}_0}{\partial \zeta} \, \mathrm{d}\zeta. \tag{8.12}$$

Now

$$\int_{-\infty}^{\infty} \tilde{g}_0 \frac{\partial \tilde{\phi}_0}{\partial \zeta} \, \mathrm{d}\zeta = \kappa, \tag{8.13}$$

https://doi.org/10.1017/jfm.2013.521 Published online by Cambridge University Press

shown in appendix C, and thus matching to the outer region gives the interface conditions

$$\boldsymbol{n}\cdot[\boldsymbol{\tau}_0^+ - \boldsymbol{\tau}_0^-]\cdot(\boldsymbol{I}-\boldsymbol{n}\otimes\boldsymbol{n}) = 0, \tag{8.14a}$$

$$\boldsymbol{n}\cdot[(-p_0^+ + p_0^-)\boldsymbol{I} + \boldsymbol{\tau}_0^+ - \boldsymbol{\tau}_0^-]\cdot\boldsymbol{n} = -\frac{\kappa}{Ca}, \tag{8.14b}$$

which are the classical stress conditions, as in figure 1.

8.3. *Extension to the tensorial mobility form*

In the work of Gugenberger *et al.* (2008) for phase field models of surface diffusion, where coupling to hydrodynamics is not considered, the tensorial form considered in the previous subsection does not recover the classical boundary conditions for their case because the leading-order outer solution is not unique. In our case the hydrodynamic coupling overcame this feature, but it is of interest to note that the more complex mobility will also recover the same results as for the tensorial form already considered.

This more complex form is

$$\gamma = \gamma_T\left(\boldsymbol{I} - 2Cn^2\frac{|\nabla\phi|^2}{(\phi^2-1)^2}(\hat{\boldsymbol{n}}\otimes\hat{\boldsymbol{n}})\right)^m = \gamma_T\left(\boldsymbol{I} - 2Cn^2\frac{\nabla\phi\otimes\nabla\phi}{(\phi^2-1)^2}\right)^m, \tag{8.15}$$

for $m\in\mathbb{Z}_+$. The analysis follows the previous form, since in the outer region this tensorial form behaves as $\gamma_T(1+O(Cn))$, so follows the CH model, and in the inner region the mobility behaves as $\boldsymbol{I}-\hat{\boldsymbol{n}}\otimes\hat{\boldsymbol{n}}(1+O(Cn^m))$, and so behaves like the previous tensorial form.

9. Concluding remarks

We have analysed a number of binary fluid models in the sharp-interface limit, allowing them to be easily compared. For one of the more prevalent models we have shown that using a tensorial mobility, where diffusion is preferred in the tangential direction to the fluid–fluid interface, allows the model to approach the classical equations asymptotically to all orders in the Cahn number, rather than non-classical terms entering at $O(Cn)$. Binary fluid models are of great use in a variety of applications, but in particular to flows with contact lines. The asymptotic behaviour in the sharp-interface limit remains an open problem for the moving contact line in this situation, with numerical work such as that by Yue *et al.* (2010) showing interesting results to compare these models to slip-based models with a sharp interface between fluids, where asymptotic analysis has been performed by Cox (1986) in the Stokes flow regime for small capillary number, and extended for non-zero Reynolds number flow (Cox 1998).

Analysis for the liquid–gas problem for contact line motion has recently been considered (Sibley *et al.* 2013) in the sharp-interface limit, building on the work of Seppecher (1996), who investigated the contact line region numerically. In the study by Sibley *et al.* (2013) it was shown that many of the features of one of the more complex continuum mechanical models for flows with the interface formation of Shikhmurzaev (2008) (and analysed recently by Sibley, Savva & Kalliadasis 2012) were reproducible by the liquid–gas diffuse-interface model. It is of interest to understand the asymptotic behaviour of the contact line in this binary fluid setting and to understand how it compares to other models suggested for resolution of the moving contact line problem.

https://doi.org/10.1017/jfm.2013.521 Published online by Cambridge University Press

Other problems of note for application of these models include wetting on heterogeneous substrates and flows through porous media. Work on these subjects with sharp-interface models has been performed by Savva, Kalliadasis & Pavliotis (2010), Vellingiri, Savva & Kalliadasis (2011) and Savva & Kalliadasis (2013) and with phase field models by Queralt-Martín *et al.* (2011), Schmuck *et al.* (2012) and Wylock *et al.* (2012). Coupling of the latter strongly diffusive regime models to hydrodynamics would be of particular interest. We should also note that the behaviour of droplets on superhydrophobic substrates caused by topographical substrate heterogeneities, an important application of wetting and multiphase flows, has been investigated with numerical computations using van der Waals theory and lattice Boltzmann solvers (closely related to phase field models) by Dupuis & Yeomans (2005), Biben & Joly (2008) and Kusumaatmaja *et al.* (2008).

Finally, we note that we have investigated a number of different mobility forms in this study. Future work to understand these forms using physical reasoning from the microscale is thus of crucial importance.

Acknowledgements

We thank the anonymous referees for useful comments and suggestions, and we acknowledge financial support from European Research Council (ERC) Advanced grant 247031 and Imperial College through a DTG International Studentship. We are grateful to Dr B. Goddard for stimulating discussions on the Fredholm alternative.

Appendix A

Another means to highlight the comparison between the way in which the various models considered here augment the momentum balance of the Navier–Stokes equations is to note that all models can be written as having the body force $g\nabla\phi/Ca$ as in the CH model, but with modified pressures $\bar{p}$. For the interested reader, this is given in table 1.

Appendix B

B.1. *Leading-order phase field solution*

The leading-order phase field is given by a solution of (3.42). This has a general solution in terms of elliptic functions given by

$$\tilde{\phi}_0 = A(\zeta^1, t)\sqrt{\frac{2}{1+A(\zeta^1,t)^2}}\; sn\left(\left.\frac{\zeta + B(\zeta^1,t)\sqrt{2}}{\sqrt{1+A(\zeta^1,t)^2}}\right| A(\zeta^1,t)\right), \tag{B 1}$$

where $sn(z|m)$ is the Jacobi elliptic function sn, and A and B must be found through the boundary or matching conditions (here $\tilde{\phi}_0|_{\zeta=0} = 0$, $\tilde{\phi}_0|_{\zeta=\pm\infty} = \pm 1$). Note that the ordinary differential equation $w''(z) - w(z)(2mw(z)^2 - m - 1) = 0$ has solution $w(z) = sn(z|m)$, which on applying $m = 1$ and the change of variable $z = x/\sqrt{2}$ gives $w'' + w(1 - w^2) = 0$, and the solution $w = sn(x/\sqrt{2}|1)$.

Whilst this elliptic function form may be useful in certain circumstances, we can obtain the solution (3.43), relevant to our situation, more easily by returning to the original equation in (3.42), and noting that $\partial_{\tilde{\phi}_0}[(\partial_\zeta\tilde{\phi}_0)^2] = 2\partial^2_\zeta\tilde{\phi}_0$, so that the equation

https://doi.org/10.1017/jfm.2013.521 Published online by Cambridge University Press

https://doi.org/10.1017/jfm.2013.521 Published online by Cambridge University Press

Model	Modified pressure, $\bar{p}$	Non-dimensional mobility
CH	p	β
Phase field dependent mobility	p	$\beta(1-\phi^2)$ or $\beta(1-\phi^2)^2$
Allen–Cahn (non-conservative)	p	α
$\phi\nabla g$ body force	$p-\dfrac{\phi g}{\mathrm{Ca}}$	β
Jacqmin (1999)	$p+\dfrac{3\sqrt{2}}{16Ca}\left[\dfrac{(\phi^2-1)^2}{Cn}-2Cn\lvert\nabla\phi\rvert^2\right]$	β
Khatavkar *et al.* (2006, 2007)	$p+\dfrac{3\sqrt{2}}{16Ca}\left[\dfrac{(\phi^2-1)^2}{Cn}+2Cn\lvert\nabla\phi\rvert^2\right]$	β
Anderson *et al.* (1998)	$p+\dfrac{3\sqrt{2}}{16Ca}\left[\dfrac{(\phi^2-1)^2}{Cn}\right]$	β
Tensorial mobility	p	$\beta(\boldsymbol{I}-\hat{\boldsymbol{n}}\otimes\hat{\boldsymbol{n}})$

TABLE 1. Summary of models analysed through formulation as a modified pressure.

becomes

$$-\frac{1}{2}\left(\frac{\partial\tilde{\phi}_0}{\partial\zeta}\right)^2+\frac{1}{4}\tilde{\phi}_0^2(\tilde{\phi}_0^2-2)=A=-\frac{1}{4}, \tag{B 2}$$

where the arbitrary constant of integration has been found using $\lim_{\zeta\to\pm\infty}\tilde{\phi}_0\to\pm1$ with $\lim_{\zeta\to\pm\infty}\partial_\zeta\tilde{\phi}_0\to0$. This leaves the equation

$$-\left(\frac{\partial\tilde{\phi}_0}{\partial\zeta}\right)^2+\frac{1}{2}(\tilde{\phi}_0^2-1)^2=0, \tag{B 3}$$

with solution

$$\tilde{\phi}_0=\tanh\left(\frac{\zeta}{\sqrt{2}}+B(\zeta^1,t)\right), \tag{B 4}$$

corresponding to the case where $A(\zeta^1,t)=1$ in the general solution (B 1), and on applying $\tilde{\phi}_0|_{\zeta=0}=0$ gives (3.43).

B.2. *Solvability condition for* $\tilde{\phi}_1$

For succinctness in the main text a fortuitous multiplication and integration was performed to obtain a solvability condition for (3.44), allowing technical details to be circumvented. Here we show how this is motivated by invoking the Fredholm alternative (Fredholm 1903).

Returning to (3.44), we notice that it may be considered as a linear inhomogeneous differential equation for $\tilde{\phi}_1$, as

$$\mathfrak{L}(\tilde{\phi}_1)=\left(\frac{\partial^2}{\partial\zeta^2}-(3\tilde{\phi}_0^2-1)\right)(\tilde{\phi}_1)=\kappa\frac{\partial\tilde{\phi}_0}{\partial\zeta}-\frac{4}{3\sqrt{2}}\tilde{g}_B. \tag{B 5}$$

The linear operator $\mathfrak{L}$ is Hermitian, since for a general second-order operator

$$\mathfrak{L}u\equiv p_0u''+p_1u'+p_2u \tag{B 6}$$

to be Hermitian, it is equal to

$$\begin{aligned}\mathfrak{L}^\dagger u&\equiv(p_0u)''+(p_1u)'+p_2u\\&=p_0u''+\left(2p_0'-p_1\right)u'+u\left(p_0''-p_1'+p_2\right).\end{aligned} \tag{B 7}$$

This occurs if $p_1=p_0'$, which is true in our case since $p_0=1$, $p_1=0$, $p_2=-(3\tilde{\phi}_0^2-1)$. Thus by the Fredholm alternative the solvability condition for (3.44) depends on the null space of the adjoint of $\mathfrak{L}$. To find this, consider

$$\mathfrak{L}^\dagger(\tilde{\phi}_1)=\mathfrak{L}(\tilde{\phi}_1)=\frac{\partial^2\tilde{\phi}_1}{\partial\zeta^2}-(3\tilde{\phi}_0^2-1)\tilde{\phi}_1=0, \tag{B 8}$$

and notice that from (3.42)

$$\frac{\partial^2\tilde{\phi}_0}{\partial\zeta^2}=\tilde{\phi}_0(\tilde{\phi}_0^2-1)\Rightarrow\frac{\partial^3\tilde{\phi}_0}{\partial\zeta^3}=(3\tilde{\phi}_0^2-1)\frac{\partial\tilde{\phi}_0}{\partial\zeta}. \tag{B 9}$$

https://doi.org/10.1017/jfm.2013.521 Published online by Cambridge University Press

Using this we find

$$\frac{\partial^2\tilde{\phi}_1}{\partial\zeta^2}\frac{\partial\tilde{\phi}_0}{\partial\zeta}=\frac{\partial^3\tilde{\phi}_0}{\partial\zeta^3}\tilde{\phi}_1\Rightarrow\frac{\partial}{\partial\zeta}\left[\frac{\partial\tilde{\phi}_1}{\partial\zeta}\frac{\partial\tilde{\phi}_0}{\partial\zeta}-\frac{\partial^2\tilde{\phi}_0}{\partial\zeta^2}\tilde{\phi}_1\right]=0, \tag{B 10}$$

and integrating this once and removing the arbitrary constant, as derivatives of $\tilde{\phi}_0$ are 0 as $\zeta\to\infty$, we obtain a separable first-order equation for $\tilde{\phi}_1$, with solution $\tilde{\phi}_1=A_s\partial_\zeta\tilde{\phi}_0$, where A_s is another arbitrary constant. This is now sufficient for us to determine the solvability condition given in (3.50).

Appendix C

Details of some calculations in § 8 are given here. The Cahn–Hilliard type equation at $O(1)$ in the outer region is calculated as

$$\begin{aligned}0&=\frac{1}{Cn}\nabla\cdot\left\{\left(\boldsymbol{I}-\frac{\nabla(\phi_0^\pm+Cn\phi_1^\pm+\cdots)\otimes\nabla(\phi_0^\pm+Cn\phi_1^\pm+\cdots)}{|\nabla(\phi_0^\pm+Cn\phi_1^\pm+\cdots)|^2}\right)\right.\\&\quad\left.\times\left[(3\phi_0^{\pm2}-1)\nabla\phi_0^\pm+Cn\left((3\phi_0^{\pm2}-1)\nabla\phi_1^\pm+6\phi_0^\pm\phi_1^\pm\nabla\phi_0^\pm\right)+O(Cn^2)\right]\right\}\\&=\frac{1}{Cn}\nabla\cdot\left\{\left(\boldsymbol{I}-\frac{\nabla\phi_1^\pm\otimes\nabla\phi_1^\pm}{|\nabla\phi_1^\pm|^2}+O(Cn)\right)\left[Cn(3\phi_0^{\pm2}-1)\nabla\phi_1^\pm+O(Cn^2)\right]\right\}\\&=\nabla\cdot\left\{\left(\boldsymbol{I}-\frac{\nabla\phi_1^\pm\otimes\nabla\phi_1^\pm}{|\nabla\phi_1^\pm|^2}\right)2\nabla\phi_1^\pm\right\}+O(Cn)\\&=O(Cn),\end{aligned} \tag{C 1}$$

the last equality following as for the leading-order case, since for a generic function ψ

$$\left(\boldsymbol{I}-\frac{\nabla\psi\otimes\nabla\psi}{|\nabla\psi|^2}\right)\nabla\psi=\boldsymbol{0}. \tag{C 2}$$

The vector $\boldsymbol{\lambda}$ appearing in the inner region analysis of the Cahn–Hilliard equation is

$$\begin{aligned}\boldsymbol{\lambda}&=\left(\boldsymbol{I}-\frac{\nabla\phi\otimes\nabla\phi}{|\nabla\phi|^2}\right)\nabla g\\&=\left[\begin{pmatrix}\dfrac{1}{(1-\kappa Cn\,\zeta)^2}&0\\0&1\end{pmatrix}-\frac{\begin{pmatrix}\left(\dfrac{\partial_{\zeta^1}\phi}{(1-\kappa Cn\,\zeta)^2}\right)^2&\dfrac{(\partial_{\zeta^1}\phi)(\partial_\zeta\phi)}{Cn(1-\kappa Cn\,\zeta)^2}\\\dfrac{(\partial_{\zeta^1}\phi)(\partial_\zeta\phi)}{Cn(1-\kappa Cn\,\zeta)^2}&\left(\dfrac{1}{Cn}\dfrac{\partial\phi}{\partial\zeta}\right)^2\end{pmatrix}}{(1-\kappa Cn\,\zeta)^{-2}\left(\partial_{\zeta^1}\phi\right)^2+Cn^{-2}\left(\partial_\zeta\phi\right)^2}\right]\\&\quad\times\begin{pmatrix}\dfrac{\partial_{\zeta^1}g}{(1-\kappa Cn\,\zeta)^2}\\\dfrac{1}{Cn}\dfrac{\partial g}{\partial\zeta}\end{pmatrix},\end{aligned} \tag{C 3}$$

https://doi.org/10.1017/jfm.2013.521 Published online by Cambridge University Press

and using expansions (3.29), we can thus expand $\boldsymbol{\lambda}$ in orders of Cn to obtain

$$\begin{aligned}
\boldsymbol{\lambda} &= \left[\begin{pmatrix} 1+2Cn\,\kappa\zeta+O(Cn^2) & 0 \\ 0 & 1 \end{pmatrix} - \left\{\left(\frac{\partial\tilde{\phi}_0}{\partial\zeta}\right)^{-2} - 2Cn\frac{\partial_\zeta\tilde{\phi}_1}{(\partial_\zeta\tilde{\phi}_0)^3}+O(Cn^2)\right\}\boldsymbol{\mathfrak{B}}\right] \\
&\quad\times\begin{pmatrix} \dfrac{\partial\tilde{g}_0}{\partial\zeta^1}+Cn\left(\dfrac{\partial\tilde{g}_1}{\partial\zeta^1}+2\kappa\zeta\dfrac{\partial\tilde{g}_0}{\partial\zeta^1}\right)+O(Cn^2) \\ \dfrac{1}{Cn}\dfrac{\partial\tilde{g}_0}{\partial\zeta}+\dfrac{\partial\tilde{g}_1}{\partial\zeta}+Cn\dfrac{\partial\tilde{g}_2}{\partial\zeta}+O(Cn^2) \end{pmatrix} \\
&= \frac{1}{Cn}\begin{pmatrix} 1 & 0 \\ 0 & 0 \end{pmatrix}\begin{pmatrix} 0 \\ \partial_\zeta\tilde{g}_0 \end{pmatrix} \\
&\quad+\left[\begin{pmatrix} 2\kappa\zeta & 0 \\ 0 & 0 \end{pmatrix} - \begin{pmatrix} 0 & \dfrac{\partial_{\zeta^1}\tilde{\phi}_0\partial_\zeta\tilde{\phi}_0}{(\partial_\zeta\tilde{\phi}_0)^2} \\ \dfrac{\partial_{\zeta^1}\tilde{\phi}_0\partial_\zeta\tilde{\phi}_0}{(\partial_\zeta\tilde{\phi}_0)^2} & -2\dfrac{\partial_\zeta\tilde{\phi}_1(\partial_\zeta\tilde{\phi}_0)^2}{(\partial_\zeta\tilde{\phi}_0)^3}+2\dfrac{\partial_\zeta\tilde{\phi}_0\partial_\zeta\tilde{\phi}_1}{(\partial_\zeta\tilde{\phi}_0)^2} \end{pmatrix}\right]\begin{pmatrix} 0 \\ \partial_\zeta\tilde{g}_0 \end{pmatrix} \\
&\quad+\begin{pmatrix} 1 & 0 \\ 0 & 0 \end{pmatrix}\begin{pmatrix} \partial_{\zeta^1}\tilde{g}_0 \\ \partial_\zeta\tilde{g}_1 \end{pmatrix}+O(Cn) \\
&= \frac{1}{Cn}\begin{pmatrix} 0 \\ 0 \end{pmatrix}+\begin{pmatrix} 2\kappa\zeta & -\left(\dfrac{\partial\tilde{\phi}_0}{\partial\zeta}\right)^{-1}\dfrac{\partial\tilde{\phi}_0}{\partial\zeta^1} \\ -\left(\dfrac{\partial\tilde{\phi}_0}{\partial\zeta}\right)^{-1}\dfrac{\partial\tilde{\phi}_0}{\partial\zeta^1} & 0 \end{pmatrix}\begin{pmatrix} 0 \\ \partial_\zeta\tilde{g}_0 \end{pmatrix} \\
&\quad+\begin{pmatrix} 1 & 0 \\ 0 & 0 \end{pmatrix}\begin{pmatrix} \partial_{\zeta^1}\tilde{g}_0 \\ \partial_\zeta\tilde{g}_1 \end{pmatrix}+O(Cn) \\
&= \begin{pmatrix} -\left(\dfrac{\partial\tilde{\phi}_0}{\partial\zeta}\right)^{-1}\dfrac{\partial\tilde{\phi}_0}{\partial\zeta^1}\dfrac{\partial\tilde{g}_0}{\partial\zeta} \\ 0 \end{pmatrix}+\begin{pmatrix} \dfrac{\partial\tilde{g}_0}{\partial\zeta^1} \\ 0 \end{pmatrix}+O(Cn), \qquad \text{(C 4)}
\end{aligned}$$

where

$$\boldsymbol{\mathfrak{B}}_{11} = O(Cn^2), \qquad \text{(C 5}a\text{)}$$

$$\boldsymbol{\mathfrak{B}}_{12} = \boldsymbol{\mathfrak{B}}_{21} = Cn\frac{\partial\tilde{\phi}_0}{\partial\zeta^1}\frac{\partial\tilde{\phi}_0}{\partial\zeta}+O(Cn^2), \qquad \text{(C 5}b\text{)}$$

$$\boldsymbol{\mathfrak{B}}_{22} = \left(\frac{\partial\tilde{\phi}_0}{\partial\zeta}\right)^2+2Cn\frac{\partial\tilde{\phi}_0}{\partial\zeta}\frac{\partial\tilde{\phi}_1}{\partial\zeta}+O(Cn^2). \qquad \text{(C 5}c\text{)}$$

https://doi.org/10.1017/jfm.2013.521 Published online by Cambridge University Press

Finally, in the analysis of the inner region momentum equations we use

$$\int_{-\infty}^{\infty} \tilde{g}_0 \frac{\partial \tilde{\phi}_0}{\partial \zeta}\,\mathrm{d}\zeta = \int_{-\infty}^{\infty} \frac{3\sqrt{2}}{4}\left\{\tilde{\phi}_1(3\tilde{\phi}_0^2-1) - \left(\frac{\partial^2 \tilde{\phi}_1}{\partial \zeta^2} - \kappa \frac{\partial \tilde{\phi}_0}{\partial \zeta}\right)\right\}\frac{\partial \tilde{\phi}_0}{\partial \zeta}\,\mathrm{d}\zeta$$

$$= \frac{3\sqrt{2}}{4}\left\{\int_{-\infty}^{\infty}\left[\tilde{\phi}_1(3\tilde{\phi}_0^2-1)\frac{\partial \tilde{\phi}_0}{\partial \zeta} - \frac{\partial^2 \tilde{\phi}_1}{\partial \zeta^2}\frac{\partial \tilde{\phi}_0}{\partial \zeta}\right]\mathrm{d}\zeta + \int_{-\infty}^{\infty}\kappa\left(\frac{\partial \tilde{\phi}_0}{\partial \zeta}\right)^2\mathrm{d}\zeta\right\}$$

$$= \frac{3\sqrt{2}}{4}\int_{-\infty}^{\infty}\kappa\left(\frac{\partial \tilde{\phi}_0}{\partial \zeta}\right)^2\mathrm{d}\zeta = \kappa. \tag{C 6}$$

REFERENCES

ALLEN, S. M. & CAHN, J. W. 1979 A microscopic theory for antiphase boundary motion and its application to antiphase domain coarsening. *Acta Metall.* **27** (6), 1085–1095.

ANDERSON, D. M., MCFADDEN, G. B. & WHEELER, A. A. 1998 Diffuse-interface methods in fluid mechanics. *Annu. Rev. Fluid Mech.* **30**, 139–165.

ANDERSON, D., MCFADDEN, G. & WHEELER, A. 2001 A phase-field model with convection: sharp-interface asymptotics. *Physica* D **151** (2–4), 305–331.

ANTANOVSKII, L. K. 1995 A phase field model of capillarity. *Phys. Fluids* **7** (4), 747–753.

BIBEN, T. & JOLY, L. 2008 Wetting on nanorough surfaces. *Phys. Rev. Lett.* **100**, 186103.

BIBEN, T., MISBAH, C., LEYRAT, A. & VERDIER, C. 2003 An advected-field approach to the dynamics of fluid interfaces. *Europhys. Lett.* **63** (4), 623.

CAGINALP, G. & FIFE, P. C. 1988 Dynamics of layered interfaces arising from phase boundaries. *SIAM J. Appl. Maths* **48** (3), 506–518.

CAHN, J. W. & HILLIARD, J. E. 1958 Free energy of a non-uniform system. Part 1. Interfacial free energy. *J. Chem. Phys.* **28** (2), 258–267.

COX, R. G. 1986 The dynamics of the spreading of liquids on a solid surface. Part 1. Viscous flow. *J. Fluid Mech.* **168**, 169–194.

COX, R. G. 1998 Inertial and viscous effects on dynamic contact angles. *J. Fluid Mech.* **357**, 249–278.

DING, H. & SPELT, P. D. M. 2007 Wetting condition in diffuse interface simulations of contact line motion. *Phys. Rev.* E **75**, 046708.

DING, H., SPELT, P. D. M. & SHU, C. 2007 Diffuse interface model for incompressible two-phase flows with large density ratios. *J. Comput. Phys.* **226** (2), 2078–2095.

DUPUIS, A. & YEOMANS, J. M. 2005 Modeling droplets on superhydrophobic surfaces: equilibrium states and transitions. *Langmuir* **21** (6), 2624–2629.

EGGERS, J. 1997 Nonlinear dynamics and breakup of free-surface flows. *Rev. Mod. Phys.* **69**, 865–930.

FOLCH, R., CASADEMUNT, J., HERNÁNDEZ-MACHADO, A. & RAMÍREZ-PISCINA, L. 1999 Phase-field model for Hele-Shaw flows with arbitrary viscosity contrast. Part 1. Theoretical approach. *Phys. Rev.* E **60**, 1724–1733.

FREDHOLM, I. 1903 Sur une classe d'équations fonctionnelles. *Acta Mathematica* **27**, 365–390.

GUGENBERGER, C., SPATSCHEK, R. & KASSNER, K. 2008 Comparison of phase-field models for surface diffusion. *Phys. Rev.* E **78**, 016703.

HOHENBERG, P. C. & HALPERIN, B. I. 1977 Theory of dynamic critical phenomena. *Rev. Mod. Phys.* **49**, 435–479.

JACQMIN, D. 1999 Calculation of two-phase Navier–Stokes flows using phase-field modeling. *J. Comput. Phys.* **155** (1), 96–127.

JACQMIN, D. 2000 Contact-line dynamics of a diffuse fluid interface. *J. Fluid Mech.* **402**, 57–88.

JIANG, W., BAO, W., THOMPSON, C. V. & SROLOVITZ, D. J. 2012 Phase field approach for simulating solid-state dewetting problems. *Acta Materialia* **60** (15), 5578–5592.

https://doi.org/10.1017/jfm.2013.521 Published online by Cambridge University Press

KHATAVKAR, V. V., ANDERSON, P. D. & MEIJER, H. E. H. 2006 On scaling of diffuse-interface models. *Chem. Engng Sci.* **61** (8), 2364–2378.

KHATAVKAR, V. V., ANDERSON, P. D. & MEIJER, H. E. H. 2007 Capillary spreading of a droplet in the partially wetting regime using a diffuse-interface model. *J. Fluid Mech.* **572**, 367–387.

KIM, J. 2012 Phase-field models for multi-component fluid flows. *Commun. Comput. Phys.* **12** (3), 613–661.

KORTEWEG, D. 1901 Sur la forme que prennent les équations du mouvement des fluides si l'on tient compte des forces capillaires causées par des variations de densité considérables mais continues et sur la théorie de la capillarité dans l'hypothèse d'une variation continue de la densité. *Arch. Néerl. des Sci. Exactes Nat. Ser.* II **6**, 1–24.

KUSUMAATMAJA, H., BLOW, M. L., DUPUIS, A. & YEOMANS, J. M. 2008 The collapse transition on superhydrophobic surfaces. *Europhys. Lett.* **81** (3), 36003.

LAPLACE, P.-S. 1805 *Traité de Mécanique Céleste*, vol. 4, Courcier.

LE ROY, S., SØNDERGÅRD, E., NERBØ, I. S., KILDEMO, M. & PLAPP, M. 2010 Diffuse-interface model for nanopatterning induced by self-sustained ion-etch masking. *Phys. Rev.* B **81**, 161401(R).

LIU, C. & SHEN, J. 2003 A phase field model for the mixture of two incompressible fluids and its approximation by a Fourier-spectral method. *Physica* D **179** (3–4), 211–228.

LOWENGRUB, J. & TRUSKINOVSKY, L. 1998 Quasi-incompressible Cahn–Hilliard fluids and topological transitions. *Proc. R. Soc. Lond.* A **454** (1978), 2617–2654.

MAGALETTI, F., PICANO, F., CHINAPPI, M., MARINO, L. & CASCIOLA, C. M. 2013 The sharp-interface limit of the Cahn–Hilliard/Navier–Stokes model for binary fluids. *J. Fluid Mech.* **714**, 95–126.

NICOLI, M., PLAPP, M. & HENRY, H. 2011 Tensorial mobilities for accurate solution of transport problems in models with diffuse interfaces. *Phys. Rev.* E **84**, 046707.

PEGO, R. L. 1989 Front migration in the nonlinear Cahn–Hilliard equation. *Proc. R. Soc. Lond.* A **422** (1863), 261–278.

PISMEN, L. M. & POMEAU, Y. 2000 Disjoining potential and spreading of thin liquid layers in the diffuse-interface model coupled to hydrodynamics. *Phys. Rev.* E **62**, 2480–2492.

QIAN, T., WANG, X.-P. & SHENG, P. 2006 A variational approach to moving contact line hydrodynamics. *J. Fluid Mech.* **564**, 333–360.

QUERALT-MARTÍN, M., PRADAS, M., RODRÍGUEZ-TRUJILLO, R., ARUNDELL, M., CORVERA POIRÉ, E. & HERNÁNDEZ-MACHADO, A. 2011 Pinning and avalanches in hydrophobic microchannels. *Phys. Rev. Lett.* **106**, 194501.

ROWLINSON, J. S. 1979 The thermodynamic theory of capillarity under the hypothesis of a continuous variation of density. *J. Stat. Phys.* **20**, 200–244 Translation of the work of J. D. van der Waals.

SAVVA, N. & KALLIADASIS, S. 2013 Droplet motion on inclined heterogeneous substrates. *J. Fluid Mech.* **725**, 462–491.

SAVVA, N., KALLIADASIS, S. & PAVLIOTIS, G. A. 2010 Two-dimensional droplet spreading over random topographical substrates. *Phys. Rev. Lett.* **104**, 084501.

SCARDOVELLI, R. & ZALESKI, S. 1999 Direct numerical simulation of free-surface and interfacial flow. *Annu. Rev. Fluid Mech.* **31** (1), 567–603.

SCHMUCK, M., PRADAS, M., PAVLIOTIS, G. A. & KALLIADASIS, S. 2012 Upscaled phase-field models for interfacial dynamics in strongly heterogeneous domains. *Proc. R. Soc. Lond.* A **468** (2147), 3705–3724.

SEPPECHER, P. 1996 Moving contact lines in the Cahn–Hilliard theory. *Intl J. Engng Sci.* **34** (9), 977–992.

SHIKHMURZAEV, Y. D. 2008 *Capillary Flows with Forming Interfaces*. Chapman & Hall/CRC.

SIBLEY, D. N., NOLD, A., SAVVA, N. & KALLIADASIS, S. 2013 On the moving contact line singularity: Asymptotics of a diffuse-interface model. *Eur. Phys. J.* E **36**, 26.

SIBLEY, D. N., SAVVA, N. & KALLIADASIS, S. 2012 Slip or not slip? A methodical examination of the interface formation model using two-dimensional droplet spreading on a horizontal planar substrate as a prototype system. *Phys. Fluids* **24** (8), 082105.

https://doi.org/10.1017/jfm.2013.521 Published online by Cambridge University Press

STAROVOITOV, V. 1994 Model of the motion of a two-component liquid with allowance of capillary forces. *J. Appl. Mech. Tech. Phys.* **35**, 891–897.

SWIFT, M. R., ORLANDINI, E., OSBORN, W. R. & YEOMANS, J. M. 1996 Lattice Boltzmann simulations of liquid–gas and binary fluid systems. *Phys. Rev.* E **54**, 5041–5052.

VELLINGIRI, R., SAVVA, N. & KALLIADASIS, S. 2011 Droplet spreading on chemically heterogeneous substrates. *Phys. Rev.* E **84**, 036305.

VILLANUEVA, W., BOETTINGER, W. J., MCFADDEN, G. B. & WARREN, J. A. 2012 A diffuse-interface model of reactive wetting with intermetallic formation. *Acta Mater.* **60** (9), 3799–3814.

VAN DER WAALS, J. D. 1893 Thermodynamische theorie der capillariteit in de onderstelling van continue dichtheidsverandering. *Verh. K. Akad. Wet. Amsterdam* **1**, 1–56.

WYLOCK, C., PRADAS, M., HAUT, B., COLINET, P. & KALLIADASIS, S. 2012 Disorder-induced hysteresis and nonlocality of contact line motion in chemically heterogeneous microchannels. *Phys. Fluids* **24** (3), 032108.

YANG, X., FENG, J. J., LIU, C. & SHEN, J. 2006 Numerical simulations of jet pinching-off and drop formation using an energetic variational phase-field method. *J. Comput. Phys.* **218** (1), 417–428.

YEON, D.-H., CHA, P.-R. & GRANT, M. 2006 Phase field model of stress-induced surface instabilities: surface diffusion. *Acta Mater.* **54** (6), 1623–1630.

YOUNG, T. 1805 An essay on the cohesion of fluids. *Phil. Trans. R. Soc. Lond.* **95**, 65–87.

YUE, P., FENG, J. J., LIU, C. & SHEN, J. 2004 A diffuse-interface method for simulating two-phase flows of complex fluids. *J. Fluid Mech.* **515**, 293–317.

YUE, P., ZHOU, C. & FENG, J. J. 2010 Sharp-interface limit of the Cahn–Hilliard model for moving contact lines. *J. Fluid Mech.* **645**, 279–294.

YUE, P., ZHOU, C., FENG, J. J., OLLIVIER-GOOCH, C. F. & HU, H. H. 2006 Phase-field simulations of interfacial dynamics in viscoelastic fluids using finite elements with adaptive meshing. *J. Comput. Phys.* **219** (1), 47–67.

https://doi.org/10.1017/jfm.2013.521 Published online by Cambridge University Press